

Nearby active galactic nuclei and starburst galaxies as sources of the measured UHECRs anisotropy signal

Cainã de Oliveira and Vitor de Souza

Instituto de Física de São Carlos, Universidade de São Paulo, Av. Trabalhador São-carlense 400, São Carlos, Brasil.

E-mail: caina.oliveira@usp.br, vitor@ifsc.usp.br

Abstract. The Pierre Auger and the Telescope Array observatories have measured independent and statistical significant anisotropy in the arrival direction of ultra-high-energy cosmic rays (UHECR). Three hotspot regions with relative excess of events and a dipole signal have been identified in different regions of the sky and energy ranges. In this paper, we investigate the conditions under which these anisotropy signal could be generated by nearby (<23 Mpc) active galactic nuclei (AGN) and/or starburst galaxies (SBG). We studied a wide range of possibilities including injected nuclei (p, He, N, Si, and Fe), three UHECR luminosity proxies and three extragalactic magnetic field models. The results shows that both local AGN and SBG are needed to describe all the anisotropy signal. The contribution of AGN to hotspots and to the generation of the dipole is dominant in most cases. SBG is required only to explain the hotspot measured by the Telescope Array Observatory.

Contents

1	Introduction	1
2	Method	3
2.1	Source selection and UHECR injection	3
2.2	Extragalactic propagation	3
3	Results I: Hotspots generated by AGNs and/or SBGs	4
4	Results II: Dipole generated by AGNs and/or SBGs	5
4.1	Dipole generated by AGNs and SBGs	5
4.2	Dipole generated only by SBGs	5
4.3	Dipole generated only by AGNs	6
4.3.1	Searching the AGN luminosity which best describes the dipole direction	6
5	Conclusion	6
A	Effect of the GMF over the hotspots	19

1 Introduction

The existence of ultra-high-energy cosmic rays (UHECR, with energy above 10^{18} eV = 1 EeV) has been known since the 1960s [1]. Even after decades of theoretical efforts and several dedicated experiments [2], the sources and acceleration mechanisms of these particles remain unknown [3]. The difficulty in identifying the sources is related to the large uncertainties in the data, the small number of events detected so far, and by the lack of knowledge about the cosmic magnetic fields.

The number of potential sources of UHECR is strongly restricted by the Hillas condition [4]. Among the most probably candidates are active galactic nuclei (AGNs) and starburst galaxies (SBGs) [3, 5]. The particle acceleration in AGNs has been widely studied by many authors [6–12]. The presence of relativistic jets emanating from supermassive black holes creates extreme environments in which the particle’s acceleration occurs [11, 13]. The radio galaxies, Centaurus A (Cen A, NGC 5128), Virgo A (Vir A, M87), and Fornax A (For A, NGC 1316) are the closest and most powerful nearby AGNs [14, 15].

SBGs drive nuclear outflows in the form of powerful and magnetized winds that constitute a potential site for particle acceleration [5, 16, 17]. The details about the efficiency of the superwind in accelerating particles at the highest energies is still under debate [18–21]. Besides that, SBGs have adequate environments for frequent extreme events in which particle acceleration is expected, such as gamma-ray bursts, trans-relativistic supernovae, and hypernovae [22–24].

Recently, the Pierre Auger [25] and the Telescope Array [26] Observatories have improved the UHECR data quality and have increased the number of detected events allowing precision studies. The Pierre Auger Observatory detected a large-scale dipolar modulation in the arrival direction of UHECR with energies above 4, 8, and 32 EeV [27, 28]. If events with energy above 4 EeV are analyzed, the dipole amplitude increases with energy and the statistical significance

of the signal has increased with the accumulation of more data [28–30]. The interpretations of these data favor extragalactic sources of UHECR [27]. A similar study done by the Telescope Array Collaboration reports a dipole structure compatible with isotropy and with the Auger dipole at the same time [31].

In addition to the large-scale anisotropy, the Pierre Auger and the Telescope Array Observatories detected regions in the sky with a relative excess of events. The Pierre Auger Collaboration reported two hotspots regions (HS1 and HS2) for events with energy above 60 EeV [32] centered approximately at $(305^\circ, 25^\circ)$ and $(290^\circ, -70^\circ)$ [33] in galactic coordinates. The Telescope Array Collaboration reported one hotspot (HS3) for events with energy above 57 EeV centered at $(146^\circ.7, 43^\circ.2)$ in equatorial coordinates [34]. Cen A has been considered the main candidate to explain one of the hotspot [6, 33, 35–42]. The absence of hotspots in the Vir A direction can be explained by the effect of the extragalactic magnetic fields in the propagation of the particles [33, 43]. It has been suggested that For A can increase the correlation of the Auger data with γ -ray AGN catalogs [19, 33].

The Pierre Auger Observatory and the Telescope Array data have also been compared to source catalogs. The Pierre Auger data shows a correlation with γ -ray AGN catalogs (2.7σ) and with SBGs catalogs (4.0σ) against the isotropic hypothesis [32]. The Telescope Array data is not able to discriminate between the SBG catalog and an isotropic sky [44].

Extragalactic and galactic magnetic fields (EGMF and GMF) deflect UHECR during their propagation. The lack of information about these cosmic magnetic fields represents one major barrier to determining the source [33, 43, 45–50]. Some information about the intensity of the EGMF be obtained by experimental techniques and little is known about its structure [51]. Nowadays, computational simulations have been used to infer more properties of the EGMF [48, 49, 52]. The data about the GMF are less scarce than of the EGMF and observationally driven models have been developed [53–56]. However, significant improvements are needed for a better description of the UHECR deflections in the GMF [45, 46].

UHECRs interact with background photons resulting in energy loss via e^+e^- pair production and pion photoproduction. These processes are energy-dependent and limit the maximal distance of the sources, indicating the need for nearby sources of UHECR [57–62]. The increase of the magnitude of the dipole modulation with energy also corroborates a growing contribution of nearby sources to the flux of UHECR [63]. The necessity of nearby sources has increased the expectation for an UHECR astronomy [64].

Recently, we have reported [33] that the Pierre Auger dipole above 32 EeV can be understood based on an excess of events coming from the three closest AGNs (Cen A, Vir A, and For A). In this paper we extend the analysis, examining the effects of the population of the nearest SBGs and of a combined approach of SBGs and AGNs. For the first time, we report that a scenario based alone on SBGs is unlikely to reproduce the dipole direction measured by the Pierre Auger Observatory, providing another layer of evidence for the particle’s acceleration in radio galaxies. In section 2 we present the details of source selection and computational simulation. We also discuss the energy spectrum imposed on each source. In section 3 general remarks about the angular contribution for the flux of UHECR coming from each source are discussed, including the possibility of contribution to each measured hotspot. The dipole generation in each scenario is discussed in section 4, in which we compare the dipole signal generated by SBGs only, AGNs only, and the combination of SBGs and AGNs. Finally, we conclude in section 5.

2 Method

2.1 Source selection and UHECR injection

In this work, we consider nearby AGNs and SBGs as sources of UHECR and explore the arrival direction signals generated in different EGMF and compositions. As in de Oliveira and de Souza [33] Cen A, Vir A, and For A were considered the main AGNs contributing to the anisotropic signal in the arrival direction of UHECR [6, 10, 12, 19]. The nineteen SBGs closer than 23 Mpc in the catalog used in The Pierre Auger Collaboration [32] were selected for the analysis in this work.

The sources are supposed to emit a power-law spectrum with a charge-dependent exponential cutoff [65]. The standard spectral index -2 provided by the first-order Fermi acceleration in strong shocks was used [66]. A cutoff rigidity of 50 EV was selected based on the suppression energy of the UHECR spectrum measured by the Pierre Auger Observatory [67].

The radio [14] and γ -ray [68, 69] luminosity of each galaxy were used as proxies for the UHECR luminosity (L_{CR}). The radio luminosity data at 1.4 GHz (L_{radio}) was directly taken from van Velzen et al. [14]. The γ -ray luminosity between 0.1 and 100 GeV (L_γ) was taken from [68, 69]. The γ -ray luminosity for SBGs was corrected by the updated distance values found in The Pierre Auger Collaboration [32]. The value of L_γ for For A was estimated using the photon flux and spectral index between 1 and 100 GeV published by the Fermi-LAT Collaboration ¹. Table 1 summarizes the main properties of the SBGs and AGNs used in the analysis.

2.2 Extragalactic propagation

The UHECR propagation in the extragalactic environment was simulated using the CRPropa3 framework [70]. From each source were injected 10^8 events of each proton (p), He, N, Si, and Fe nuclei with energies between 8 and 1000 EeV. In the simulations, the events are isotropically emitted by the sources with a distribution following a power-law in energy with spectral index -1 , to guarantee equal statistical fluctuations at all energies. After the detection, each particle receives an energy-dependent weight to generate the spectrum of interest [10, 33].

During the extragalactic propagation, it is necessary to take into account the interactions with background photons and the deflections due to the EGMF. The simulations include the presence of the cosmic microwave background and the extragalactic background light model of Gilmore et al. [71]. The UHECR interactions with the photon backgrounds include e^+e^- pair production, pion photoproduction, and photodisintegration. Nuclear decay and adiabatic losses are also considered.

The extragalactic magnetic field models developed by Hackstein et al. [52] were employed in the simulations. We select the same models used in de Oliveira and de Souza [33]: AstrophysicalR (AstroR), Primordial (Prim), and Primordial2R (Prim2R). These models cover a wide range of field intensity and level of structure of the EGMF.

The particles were followed until they left a box of size twice the source distance or reached the observer sphere, located in the Milky Way. To maximize the number of detected particles and keep the arrival uncertainties smaller than 1° , the radius of the detector sphere (r_{obs}) was chosen based on the distance (D) of the source ($r_{obs} = D \sin(1^\circ)$). To ensure that a representative number of events will be detected, the minimum value of r_{obs} was taken as 100 kpc. The effect of differences in the observer area on the detected flux to each source was

¹<https://www.ssdsc.asi.it/fermi3lac/>

corrected by applying a r_{obs}^{-2} weight. A discussion about the size of the observer can be found in de Oliveira and de Souza [33].

Due to its small size (~ 30 kpc) compared to the distance to extragalactic sources (\sim Mpc), the energy losses can be ignored in the interior of the Milky Way. The effect of the GMF on the arrival directions of UHECR cannot be ignored. It was accounted using a parametrization of the Jansson and Farrar [54] GMF model (JF12) [72]. Both the regular and random components of JF12 were considered, using the module GalacticLens of CRPropa 3.

3 Results I: Hotspots generated by AGNs and/or SBGs

Figure 1 shows the relative contribution of each source evaluated as L_{CR}/D^2 . NGC 253, the closest source, has its flux arbitrarily set to one. Three normalizations for the flux of energy leaving the sources are used: a) equal flux (1:1), b) radio flux, and c) γ -ray flux as explained above. The use of electromagnetic luminosities as gauges to L_{CR} changes considerably the dominant sources. In the case that L_{CR} scales with L_{radio} , the radio galaxies strongly dominate over the SBGs. If the L_{CR} scales with L_{γ} , Cen A remains the main source followed by VirA and the closest SBGs (M82 and NGC 253). Distant SBGs sources (16.3 Mpc) can have a contribution to the energy flux compared to the nearby sources if L_{radio} or L_{γ} are used as a proxy (e.g. [73]).

The influence of the EGMF model is illustrated in figure 2. NGC 253, the closest source, has its value arbitrarily set to one when the AstroR EGMF is used. The AstroR EGMF model has a very small ($< 10\%$) effect on the energy flux received on Earth as emitted by any of the sources. In this case, the closer sources have a more important contribution, being dominated by NGC 253 among the SBGs, and by Cen A among the AGNs. The Prim2R EGMF model suppresses the energy flux of NGC 5055, NGC 3628, NGC 3627, NGC 4631, M51, NGC 3556, NGC 3079, and Vir A. In the Prim EGMF model, the magnetic deflections can suppress or enhance the contribution from a source. The suppression occurs to the same sources affected by the Prim2R, in addition to M83, NGC 6946, and NGC 660. The enhancement happens to M82, NGC 4945, NGC 2903, NGC 2146, and For A.

Figures 3 and 4 shows the arrival directions map for events with energies above 60 EeV when local AGNs and SBGs were considered the sources of UHECR, respectively. The color scale indicates the number of events on a logarithm scale arriving at Earth. In each line, one EGMF model is presented. In each column, the injected nuclei are shown: proton, nitrogen, and iron. The position of the sources is shown only in the first diagram for sake of clarity. The hotspot regions measured by the Pierre Auger (HS1 and HS2) and the Telescope Array (HS3) are also shown. The majority of suppressed sources are located in regions of large ($> 60^\circ$) galactic latitudes. The effect of the GMF is discussed in the appendix A.

HS1 is populated mainly by M83 and Cen A. When light nuclei are injected (p, He, N), M83 and Cen A generate more than 95% of the events populating the HS1 as shown in figure 5. When heavier nuclei are injected (Si and Fe), NGC 4945, For A, and Vir A also contribute to HS1, but the exact contribution of each source becomes highly dependent on the EGMF model.

As shown in figure 6, the HS2 is populated primarily by NGC 253, NGC 1068, and For A. The dominant source is highly dependent on the EGMF and composition injected. Note that light nuclei (p and He) injected by these sources do not reach the HS2 location.

HS3 is mostly populated by NGC 2903 and NGC 3079 independently of the EGMF model in the case of light and intermediate composition, as shown in figure 7. In the AstroR EGMF

model, there is no significant contribution of additional sources for light and intermediate nuclei (p, He, and N). The contribution of Vir A and For A depend strongly on the EGMF model and ejected nuclei, being more important in the case of heavy nuclei (Si and Fe).

4 Results II: Dipole generated by AGNs and/or SBGs

The dipole direction generated by the simulated events was evaluated using the methodology proposed by Aublin and Parizot [74]. The partial-sky coverage of the Pierre Auger Observatory was used. Different scenarios were considered:

- Sources: only SBG, only AGN, or both SBG and AGN;
- UHECR luminosity: equal luminosity (1:1), scaling with L_{radio} , and scaling with L_{γ} ;
- EGMF models: AstroR, Prim2R, and Prim;
- Nuclei injected by the source: proton, He, N, Si or Fe;
- Energy range of the events at Earth: above 8 EeV and above 32 EeV.

In each scenario, we compare the simulated results with the Pierre Auger Observatory data [30]. Figure 8 shows the angular aperture ($\Delta\Omega$) between the simulated dipole and the dipole direction measured by the Pierre Auger Observatory considering that only AGN, only SBGs, or both AGNs and SBGs are sources of UHECR. Figure 9 show the dipole direction in sky maps corresponding to the case in which AGNs and SBGs are sources, and events with energy above 32 EeV are considered.

4.1 Dipole generated by AGNs and SBGs

When both AGNs and SBGs are sources of UHECR, the direction of the simulated dipole is highly dependent on the UHECR luminosity proxies and the injected nuclei for both energy ranges. The dependence on the composition is more extreme in the case of equal UHECR luminosity of the sources. In the case of UHECR luminosity scaling with the radio luminosity, the dipole is dictated by Cen A. When the UHECR luminosity scales with the gamma luminosity, the dipole is dictated by Cen A, M82, and NGC4945.

For the energies above 8 EeV, no combination of EGMF model, UHECR luminosity proxies and the inject nuclei could reproduce the dipole direction measured by the Pierre Auger Observatory.

For the energies above 32 EeV, if the UHECR luminosity is considered proportional to the radio luminosity, the dipole direction measured by the Pierre Auger Observatory could be described for most of the injected nuclei and for all EGMF models. When the UHECR luminosity was considered proportional to the gamma luminosity the measured dipole direction could be described in some cases when heavy nuclei were injected.

4.2 Dipole generated only by SBGs

When only SBGs are sources of UHECR, no combination of EGMF model, UHECR luminosity proxies and the inject nuclei could reproduce the dipole direction measured by the Pierre Auger Observatory, independently of the energy range considered. The dipole direction is highly dependent on the nuclei injected by the source, on the EGMF, and on the UHECR luminosity.

4.3 Dipole generated only by AGNs

When only Cen A, Vir A, and For A are UHECR sources, the dipole direction does not change significantly for the UHECR luminosity proxies considered here ($< 17^\circ$ for energies above 8 EeV; and $< 11^\circ$ for energies above 32 EeV). The dipole direction is dictated by Cen A for both energy ranges (> 8 and > 32 EeV) considered. As Cen A is a very close source, the dipole direction is not greatly affected by the EGMF model ($< 11^\circ$ for both energy ranges). In the case in which all the scenarios are compared the dipole direction changes less than 31° .

For the energies above 8 EeV, no combination of EGMF model, UHECR luminosity proxies and the inject nuclei could reproduce the dipole direction measured by the Pierre Auger Observatory.

For the energies above 32 EeV, most combinations of EGMF model, UHECR luminosity proxies and the inject nuclei could reproduce the dipole direction measured by the Pierre Auger Observatory within the uncertainties. The agreement between data and simulation does not depend on the EGMF model and UHECR luminosity proxies. The agreement between data and simulation improves with heavier nuclei.

4.3.1 Searching the AGN luminosity which best describes the dipole direction

The results presented in the previous section suggest that Cen A, Vir A, and For A can generate events to reproduce the measured direction of the dipole above 32 EeV. In this section, we allow the UHECR luminosity to vary and search for the best combination of UHECR flux coming Cen A, Vir A, and For A which reproduces the measured direction of the dipole above 32 EeV. We varied the relative contribution of Vir A and For A in relation to Cen A by a factor going from 10^{-2} to 10^2 and calculated the dipole direction.

Figures 10 and 11 show the angular distance ($\Delta\Omega$) between the simulated dipole and the measure dipole as a function of the relative contribution of Vir A (L_{VirA}) and For A (L_{ForA}) in relation to Cen A (L_{CenA}). The color code shows the angular distance in units of δ , the uncertainty on the dipole direction determined by the Pierre Auger Collaboration. If the simulated dipole is inside (outside) the uncertainty of the measure dipole then $\frac{\Delta\Omega}{\delta} < 1$ (> 1). The location of the three luminosity proxies considered in the previous sections is shown by the square (1:1:1), circle (Radio), and star (Gamma).

For the energy range above 8 EeV, the measured dipole could not be described by any combination of EGMF model, UHECR luminosity proxies, inject nuclei, and values of L_{ForA}/L_{CenA} and L_{VirA}/L_{CenA} tested here.

For the energy range above 32 EeV, the dipole can be reproduced for a large range of values of L_{ForA}/L_{CenA} and L_{VirA}/L_{CenA} if Silicon and Iron are injected for all EGMF models. If light nuclei are injected (p and He), there is a very narrow range of L_{ForA}/L_{CenA} and L_{VirA}/L_{CenA} ($\sim 10 - 100$) for which the measured dipole could be described. If a intermediary nuclei (N) is considered, the simulated dipole can describe the data only with Prim2R EGMF model and with $L_{VirA} \sim L_{ForA} \geq 25L_{CenA}$.

5 Conclusion

We investigated the measured anisotropic signal in UHECR arrival direction, namely the dipole and three hotspots, under the assumption that nearby AGNs and SBGs are the sources of these features. We studied different UHECR luminosity proxies (1:1, Radio, and Gamma), injection of several nuclei (p, He, N, Si, and Fe), and EGMF models (AstroR, Prim, and Prim2R). The importance of considering EGMF models in the study of UHECR anisotropy

was once again confirmed [33, 48, 75–78]. The dipole and the hotspots can not be interpreted without the consideration of structured EGMF models as the ones used here. Beyond the previous results, we showed here that the Prim2R EGMF model suppresses the flux arriving at Earth from several possible sources: NGC 5055, NGC 3628, NGC 3627, NGC 4631, M51, NGC 3556, NGC 3079, and Vir A. The Prim EGMF model suppresses the flux of these sources in addition to M83, NGC 6946, and NGC 660. Prim EGMF model enhancements the flux of M82, NGC 4945, NGC 2903, NGC 2146, and For A. This relative suppression/enhancement effect illustrates the importance of considering structured EGMF models in UHECR studies.

Our results suggest the hotspots measured by the Pierre Auger Observatory (HS1 and HS2) are dominated by nearby AGNs (Cen A and For A) emitting intermediate to heavy primaries (figures 5 and 6). Some SBGs (M83, NGC 253, and NGC 1068) also contribute with less importance. The HS3 is mostly populated by SBGs (NGC 2903 and NGC 3019) with a smaller contribution of Vir A, however the results are more dependent on the EGMF model and injected nuclei.

The measured dipole for energies above 8 EeV cannot be described by nearby SBG only, neither by nearby AGN only, nor by nearby AGNs and SBGs combined. The measured dipole for energies above 32 EeV can be described by nearby AGN only and cannot be described by SBG only neither by AGNs and SBGs combined.

The astrophysical model emerging from these results requires UHECR production in AGNs and SBGs. The flux on Earth would be dominated by AGNs emitting intermediate to heavy primaries. This would explain the hotspots HS1 and HS2, is consistent with composition-sensitive measurements [79] and anisotropy beyond 32 EeV measured by the Pierre Auger Observatory. SBGs would contribute to the flux on Earth at a moderate percentage which is needed to explain HS3 measured by the Telescope Array Experiment.

The dipole measured for energies above 8 EeV can not be explained by any combination of AGNs and SBGs within the scenarios explored here, including three EGMF models, three UHECRs luminosity proxies, and inject nuclei from proton to iron. The dipole for energies above 8 EeV would need an extra source component, beyond local AGNs and SBGs, to be explained. The need for an extra component has been also advocated by studies of the energy spectrum [80, 81]. Galactic sources have been considered, such as hyper-novae [82, 83], young neutron star winds [84] and magnetars [85]. In these models, the injected composition would need to be heavier nuclei otherwise the maximum energy leaving the source would not exceed 10^{18} eV. The anisotropies generated in these galactic scenarios have not been studied. Another possibility would be a further (> 20 Mpc) anomalous source for which the injected particles would arrive on Earth with energy around the photon-pion production threshold. Cygnus A can be one of these sources [10], at a distance of about 250 Mpc (inside the magnetic horizon) and a radio luminosity of 1.6×10^{44} erg/s [14], it could contribute with intermediate mass of energy below $10^{19.5}$ eV. The relative large abundancy of SBG in respect to AGNs could generate more HS than the ones current measured. This was not investigated in this paper in which we focus on the explanation of the measured anisotropy signal.

Acknowledgments

CO and VdS acknowledge FAPESP Project 2019/10151-2 and 2020/15453-4, 2021/01089-1. The authors acknowledge the National Laboratory for Scientific Computing (LNCC/MCTI, Brazil) for providing HPC resources of the SDumont supercomputer (<http://sdumont.lncc.br>).

VdS acknowledges CNPq. This study was financed in part by the Coordenação de Aperfeiçoamento de Pessoal de Nível Superior - Brasil (CAPES) - Finance Code 001.

References

- [1] John Linsley. Evidence for a primary cosmic-ray particle with energy 10^{20} ev. *Phys. Rev. Lett.*, 10:146–148, Feb 1963. doi: 10.1103/PhysRevLett.10.146. URL <https://link.aps.org/doi/10.1103/PhysRevLett.10.146>.
- [2] M. Nagano and A. A. Watson. Observations and implications of the ultrahigh-energy cosmic rays. *Rev. Mod. Phys.*, 72:689–732, Jul 2000. doi: 10.1103/RevModPhys.72.689. URL <https://link.aps.org/doi/10.1103/RevModPhys.72.689>.
- [3] Rafael Alves Batista, Jonathan Biteau, Mauricio Bustamante, Klaus Dolag, Ralph Engel, Ke Fang, Karl-Heinz Kampert, Dmitriy Kostunin, Miguel Mostafa, Kohta Murase, et al. Open questions in cosmic-ray research at ultrahigh energies. *Frontiers in Astronomy and Space Sciences*, 6:23, 2019.
- [4] A. M. Hillas. The origin of ultra-high-energy cosmic rays. *Annual Review of Astronomy and Astrophysics*, 22(1):425–444, 1984. doi: 10.1146/annurev.aa.22.090184.002233.
- [5] Kohta Murase and Masataka Fukugita. Energetics of high-energy cosmic radiations. *Phys. Rev. D*, 99:063012, Mar 2019. doi: 10.1103/PhysRevD.99.063012. URL <https://link.aps.org/doi/10.1103/PhysRevD.99.063012>.
- [6] VL Ginzburg and SI Syrovatskii. Cosmic rays in metagalactic space. *Soviet Astronomy*, 7:357, 1963.
- [7] Damiano Caprioli. “ESPRESSO” ACCELERATION OF ULTRA-HIGH-ENERGY COSMIC RAYS. *The Astrophysical Journal*, 811(2):L38, sep 2015. doi: 10.1088/2041-8205/811/2/L38. URL <https://doi.org/10.1088/2041-8205/811/2/L38>.
- [8] Ruo-Yu Liu, Frank M Rieger, and Felix A Aharonian. Particle acceleration in mildly relativistic shearing flows: The interplay of systematic and stochastic effects, and the origin of the extended high-energy emission in AGN jets. *The Astrophysical Journal*, 842(1):39, 2017.
- [9] Shigeo S. Kimura, Kohta Murase, and B. Theodore Zhang. Ultrahigh-energy cosmic-ray nuclei from black hole jets: Recycling galactic cosmic rays through shear acceleration. *Phys. Rev. D*, 97:023026, Jan 2018. doi: 10.1103/PhysRevD.97.023026. URL <https://link.aps.org/doi/10.1103/PhysRevD.97.023026>.
- [10] Björn Eichmann, Jörg P Rachen, Lukas Merten, Arjen van Vliet, and J Becker Tjus. Ultra-high-energy cosmic rays from radio galaxies. *Journal of Cosmology and Astroparticle Physics*, 2018(02):036, 2018.
- [11] James H Matthews, Anthony R Bell, Katherine M Blundell, and Anabella T Araudo. Ultrahigh energy cosmic rays from shocks in the lobes of powerful radio galaxies. *Monthly Notices of the Royal Astronomical Society*, 482(4):4303–4321, 2019.
- [12] Björn Eichmann. High energy cosmic rays from Fanaroff-Riley radio galaxies. *Journal of Cosmology and Astroparticle Physics*, 2019(05):009, 2019.
- [13] CD Dermer, S Razzaque, JD Finke, and A Atoyan. Ultra-high-energy cosmic rays from black hole jets of radio galaxies. *New Journal of Physics*, 11(6):065016, 2009.
- [14] Sjoert van Velzen, Heino Falcke, Pim Schellart, Nils Nierstenhöfer, and Karl-Heinz Kampert. Radio galaxies of the local universe: all-sky catalog, luminosity functions, and clustering. *Astronomy & Astrophysics*, 544:A18, 2012.

- [15] K. W. Cavagnolo, B. R. McNamara, P. E. J. Nulsen, C. L. Carilli, C. Jones, and L. Birzan. A Relationship Between AGN Jet Power and Radio Power. *The Astrophysical Journal*, 720(2): 1066–1072, Sep 2010. doi: 10.1088/0004-637X/720/2/1066.
- [16] L. A. Anchordoqui, G. E. Romero, and J. A. Combi. Heavy nuclei at the end of the cosmic-ray spectrum? *Phys. Rev. D*, 60:103001, Oct 1999. doi: 10.1103/PhysRevD.60.103001. URL <https://link.aps.org/doi/10.1103/PhysRevD.60.103001>.
- [17] Luis Alfredo Anchordoqui. Acceleration of ultrahigh-energy cosmic rays in starburst superwinds. *Phys. Rev. D*, 97:063010, Mar 2018. doi: 10.1103/PhysRevD.97.063010. URL <https://link.aps.org/doi/10.1103/PhysRevD.97.063010>.
- [18] Romero, G. E., Müller, A. L., and Roth, M. Particle acceleration in the superwinds of starburst galaxies. *A&A*, 616:A57, 2018. doi: 10.1051/0004-6361/201832666. URL <https://doi.org/10.1051/0004-6361/201832666>.
- [19] James H Matthews, Anthony R Bell, Katherine M Blundell, and Anabella T Araudo. Fornax A, Centaurus A, and other radio galaxies as sources of ultrahigh energy cosmic rays. *Monthly Notices of the Royal Astronomical Society: Letters*, 479(1):L76–L80, 2018.
- [20] Kumiko Kotera and Martin Lemoine. Optical depth of the universe to ultrahigh energy cosmic ray scattering in the magnetized large scale structure. *Phys. Rev. D*, 77:123003, Jun 2008. doi: 10.1103/PhysRevD.77.123003. URL <https://link.aps.org/doi/10.1103/PhysRevD.77.123003>.
- [21] A R Bell and J H Matthews. Echoes of the past: ultra-high-energy cosmic rays accelerated by radio galaxies, scattered by starburst galaxies. *Monthly Notices of the Royal Astronomical Society*, 511(1):448–456, 01 2022. ISSN 0035-8711. doi: 10.1093/mnras/stac031. URL <https://doi.org/10.1093/mnras/stac031>.
- [22] B. Theodore Zhang and Kohta Murase. Ultrahigh-energy cosmic-ray nuclei and neutrinos from engine-driven supernovae. *Phys. Rev. D*, 100:103004, Nov 2019. doi: 10.1103/PhysRevD.100.103004. URL <https://link.aps.org/doi/10.1103/PhysRevD.100.103004>.
- [23] B. Theodore Zhang, Kohta Murase, Shigeo S. Kimura, Shunsaku Horiuchi, and Peter Mészáros. Low-luminosity gamma-ray bursts as the sources of ultrahigh-energy cosmic ray nuclei. *Phys. Rev. D*, 97:083010, Apr 2018. doi: 10.1103/PhysRevD.97.083010. URL <https://link.aps.org/doi/10.1103/PhysRevD.97.083010>.
- [24] Peter L. Biermann, Laurentiu I. Caramete, Federico Fraschetti, Laszlo A. Gergely, Benjamin C. Harms, Emma Kun, Jon Paul Lundquist, Athina Meli, Biman B. Nath, Eun-Suk Seo, Todor Stanev, and Julia Becker Tjus. The nature and origin of ultra-high energy cosmic ray particles, 2016. URL <https://arxiv.org/abs/1610.00944>.
- [25] The Pierre Auger Collaboration. The Pierre Auger Cosmic Ray Observatory. *Nuclear Instruments and Methods in Physics Research Section A: Accelerators, Spectrometers, Detectors and Associated Equipment*, 798:172–213, 2015. ISSN 0168-9002. doi: <https://doi.org/10.1016/j.nima.2015.06.058>. URL <https://www.sciencedirect.com/science/article/pii/S0168900215008086>.
- [26] T. Abu-Zayyad et al. (The Telescope Array Collaboration). The surface detector array of the Telescope Array experiment. *Nuclear Instruments and Methods in Physics Research Section A: Accelerators, Spectrometers, Detectors and Associated Equipment*, 689:87–97, Oct 2012. ISSN 0168-9002. doi: 10.1016/j.nima.2012.05.079. URL <http://dx.doi.org/10.1016/j.nima.2012.05.079>.
- [27] The Pierre Auger Collaboration. Observation of a large-scale anisotropy in the arrival directions of cosmic rays above 8×10^{18} eV. *Science*, 357(6357):1266–1270, 2017. ISSN 0036-8075. doi: 10.1126/science.aan4338. URL <https://science.sciencemag.org/content/357/6357/1266>.

- [28] The Pierre Auger Collaboration. Large-scale cosmic-ray anisotropies above 4 EeV measured by the Pierre Auger Observatory. *The Astrophysical Journal*, 868(1):4, nov 2018. doi: 10.3847/1538-4357/aae689. URL <https://doi.org/10.3847/1538-4357/aae689>.
- [29] A. Aab, P. Abreu, M. Aglietta, I. F. M. Albuquerque, J. M. Albury, I. Allekotte, A. Almela, J. Alvarez Castillo, J. Alvarez-Muñiz, G. A. Anastasi, L. Anchordoqui, B. Andrada, S. Andringa, C. Aramo, P. R. Araújo Ferreira, H. Asorey, P. Assis, G. Avila, A. M. Badescu, A. Bakalova, A. Balaceanu, F. Barbato, R. J. Barreira Luz, K. H. Becker, J. A. Bellido, C. Berat, M. E. Bertaina, X. Bertou, P. L. Biermann, T. Bister, J. Biteau, A. Blanco, J. Blazek, C. Bleve, M. Boháčová, D. Boncioli, C. Bonifazi, L. Bonneau Arbeletche, N. Borodai, A. M. Botti, J. Brack, T. Bretz, F. L. Briechle, P. Buchholz, A. Bueno, S. Buitink, M. Buscemi, K. S. Caballero-Mora, L. Caccianiga, L. Calcagni, A. Cancio, F. Canfora, I. Caracas, J. M. Carceller, R. Caruso, A. Castellina, F. Catalani, G. Cataldi, L. Cazon, M. Cerda, J. A. Chinellato, K. Choi, J. Chudoba, L. Chytka, R. W. Clay, A. C. Cobos Cerutti, R. Colalillo, A. Coleman, M. R. Coluccia, R. Conceição, A. Condorelli, G. Consolati, F. Contreras, F. Convenga, C. E. Covault, S. Dasso, K. Daumiller, B. R. Dawson, J. A. Day, R. M. de Almeida, J. de Jesús, S. J. de Jong, G. De Mauro, J. R. T. de Mello Neto, I. De Mitri, J. de Oliveira, D. de Oliveira Franco, V. de Souza, J. Debatin, M. del Río, O. Deligny, N. Dhital, A. Di Matteo, M. L. Díaz Castro, C. Dobrigkeit, J. C. D’Oliveiro, Q. Dorosti, R. C. dos Anjos, M. T. Dova, J. Ebr, R. Engel, I. Epicoco, M. Erdmann, C. O. Escobar, A. Etchegoyen, H. Falcke, J. Farmer, G. Farrar, A. C. Fauth, N. Fazzini, F. Feldbusch, F. Fenu, B. Fick, J. M. Figueira, A. Filipčić, M. M. Freire, T. Fujii, A. Fuster, C. Galea, C. Galelli, B. García, A. L. Garcia Vegas, H. Gemmeke, F. Gesualdi, A. Gherghel-Lascu, P. L. Ghia, U. Giaccari, M. Giammarchi, M. Giller, J. Glombitza, F. Gobbi, G. Golup, M. Gómez Berisso, P. F. Gómez Vitale, J. P. Gongora, N. González, I. Goos, D. Góra, A. Gorgi, M. Gottowik, T. D. Grubb, F. Guarino, G. P. Guedes, E. Guido, S. Hahn, R. Halliday, M. R. Hampel, P. Hansen, D. Harari, V. M. Harvey, A. Haungs, T. Hebbeker, D. Heck, G. C. Hill, C. Hojvat, J. R. Hörandel, P. Horvath, M. Hrabovský, T. Huege, J. Hulsman, A. Insolia, P. G. Isar, J. A. Johnsen, J. Jurysek, A. Kääpä, K. H. Kampert, B. Keilhauer, J. Kemp, H. O. Klages, M. Kleifges, J. Kleinfeller, M. Köpke, G. Kukec Mezek, A. Kuotb Awad, B. L. Lago, D. LaHurd, R. G. Lang, M. A. Leigui de Oliveira, V. Lenok, A. Letessier-Selvon, I. Lhenry-Yvon, D. Lo Presti, L. Lopes, R. López, A. López Casado, R. Lorek, Q. Luce, A. Lucero, A. Machado Payeras, M. Malacari, G. Mancarella, D. Mandat, B. C. Manning, J. Manshanden, P. Mantsch, A. G. Mariazzi, I. C. Mariş, G. Marsella, D. Martello, H. Martinez, O. Martínez Bravo, M. Mastrodicasa, H. J. Mathes, J. Matthews, G. Matthiae, E. Mayotte, P. O. Mazur, G. Medina-Tanco, D. Melo, A. Menshikov, K.-D. Merenda, S. Michal, M. I. Micheletti, L. Miramonti, D. Mockler, S. Mollerach, F. Montanet, C. Morello, G. Morlino, M. Mostafá, A. L. Müller, M. A. Muller, S. Müller, R. Mussa, M. Muzio, W. M. Namasaka, L. Nellen, M. Niculescu-Oglinزانu, M. Niechciol, D. Nitz, D. Nosek, V. Novotny, L. Nožka, A. Nucita, L. A. Núñez, M. Palatka, J. Pallotta, M. P. Panetta, P. Papenbreer, G. Parente, A. Parra, M. Pech, F. Pedreira, J. Pekala, R. Pelayo, J. Peña-Rodriguez, L. A. S. Pereira, J. Perez Armand, M. Perlin, L. Perrone, C. Peters, S. Petretera, T. Pierog, M. Pimenta, V. Pirronello, M. Platino, B. Pont, M. Pothast, P. Privitera, M. Prouza, A. Puyleart, S. Querchfeld, J. Rautenberg, D. Ravnigani, M. Reininghaus, J. Ridky, F. Riehn, M. Risse, P. Ristori, V. Rizi, W. Rodrigues de Carvalho, J. Rodriguez Rojo, M. J. Roncoroni, M. Roth, E. Roulet, A. C. Rovero, P. Ruehl, S. J. Saffi, A. Saftoiu, F. Salamida, H. Salazar, G. Salina, J. D. Sanabria Gomez, F. Sánchez, E. M. Santos, E. Santos, F. Sarazin, R. Sarmento, C. Sarmiento-Cano, R. Sato, P. Savina, C. Schäfer, V. Scherini, H. Schieler, M. Schimassek, M. Schimp, F. Schlüter, D. Schmidt, O. Scholten, P. Schovánek, F. G. Schröder, S. Schröder, S. J. Sciutto, M. Scornavacche, R. C. Shellard, G. Sigl, G. Silli, O. Sima, R. Šmída, P. Sommers, J. F. Soriano, J. Souchard, R. Squartini, M. Stadelmaier, D. Stanca, S. Stanič, J. Stasielak, P. Stassi, A. Streich, M. Suárez-Durán, T. Sudholz, T. Suomijärvi, A. D. Supanitsky, J. Šupík, Z. Szadkowski, A. Taboada, O. A. Tabora, A. Tapia, C. Timmermans, P. Tobiska, C. J. Todero Peixoto, B. Tomé, G. Torralba Elipe, A. Travaini, P. Travnicek, C. Trimarelli, M. Trini, M. Tueros, R. Ulrich, M. Unger,

M. Urban, L. Vaclavek, J. F. Valdés Galicia, I. Valiño, L. Valore, A. van Vliet, E. Varela, B. Vargas Cárdenas, A. Vásquez-Ramírez, D. Veberič, C. Ventura, I. D. Vergara Quispe, V. Verzi, J. Vicha, L. Villaseñor, J. Vink, S. Vorobiov, H. Wahlberg, A. A. Watson, M. Weber, A. Weindl, L. Wiencke, H. Wilczyński, T. Winchen, M. Wirtz, D. Wittkowski, B. Wundheiler, A. Yushkov, E. Zas, D. Zavrtanik, M. Zavrtanik, L. Zehrer, A. Zepeda, M. Ziolkowski, and F. Zuccarello and. Cosmic-ray anisotropies in right ascension measured by the pierre auger observatory. *The Astrophysical Journal*, 891(2):142, mar 2020. doi: 10.3847/1538-4357/ab7236. URL <https://doi.org/10.3847/1538-4357/ab7236>.

- [30] The Pierre Auger Collaboration. Large-scale and multipolar anisotropies of cosmic rays detected at the Pierre Auger Observatory with energies above 4 EeV. In *Proceedings of 37th International Cosmic Ray Conference — PoS(ICRC2021)*, volume 395, page 335, 2021. doi: 10.22323/1.395.0335.
- [31] R. U. Abbasi, M. Abe, T. Abu-Zayyad, M. Allen, R. Azuma, E. Barcikowski, J. W. Belz, D. R. Bergman, S. A. Blake, R. Cady, B. G. Cheon, J. Chiba, M. Chikawa, A. di Matteo, T. Fujii, K. Fujisue, K. Fujita, R. Fujiwara, M. Fukushima, G. Furlich, W. Hanlon, M. Hayashi, N. Hayashida, K. Hibino, R. Higuchi, K. Honda, D. Ikeda, T. Inadomi, N. Inoue, T. Ishii, R. Ishimori, H. Ito, D. Ivanov, H. Iwakura, H. M. Jeong, S. Jeong, C. C. H. Jui, K. Kadota, F. Kakimoto, O. Kalashev, K. Kasahara, S. Kasami, H. Kawai, S. Kawakami, S. Kawana, K. Kawata, E. Kido, H. B. Kim, J. H. Kim, J. H. Kim, M. H. Kim, S. W. Kim, S. Kishigami, V. Kuzmin, M. Kuznetsov, Y. J. Kwon, K. H. Lee, B. Lubsandorzhev, J. P. Lundquist, K. Machida, H. Matsumiya, T. Matsuyama, J. N. Matthews, R. Mayta, M. Minamino, K. Mukai, I. Myers, S. Nagataki, K. Nakai, R. Nakamura, T. Nakamura, Y. Nakamura, Y. Nakamura, T. Nonaka, H. Oda, S. Ogio, M. Ohnishi, H. Ohoka, Y. Oku, T. Okuda, Y. Omura, M. Ono, R. Onogi, A. Oshima, S. Ozawa, I. H. Park, M. S. Pshirkov, J. Remington, D. C. Rodriguez, G. Rubtsov, D. Ryu, H. Sagawa, R. Sahara, Y. Saito, N. Sakaki, T. Sako, N. Sakurai, K. Sano, T. Seki, K. Sekino, P. D. Shah, F. Shibata, T. Shibata, H. Shimodaira, B. K. Shin, H. S. Shin, J. D. Smith, P. Sokolsky, N. Sone, B. T. Stokes, T. A. Stroman, T. Suzawa, Y. Takagi, Y. Takahashi, M. Takamura, M. Takeda, R. Takeishi, A. Taketa, M. Takita, Y. Tameda, H. Tanaka, K. Tanaka, M. Tanaka, Y. Tanoue, S. B. Thomas, G. B. Thomson, P. Tinyakov, I. Tkachev, H. Tokuno, T. Tomida, S. Troitsky, Y. Tsunesada, Y. Uchihori, S. Udo, T. Uehama, F. Urban, T. Wong, K. Yada, M. Yamamoto, K. Yamazaki, J. Yang, K. Yashiro, M. Yosei, Y. Zhezher, and Z. Zundel and. Search for large-scale anisotropy on arrival directions of ultra-high-energy cosmic rays observed with the telescope array experiment. *The Astrophysical Journal*, 898(2):L28, jul 2020. doi: 10.3847/2041-8213/aba0bc. URL <https://doi.org/10.3847/2041-8213/aba0bc>.
- [32] The Pierre Auger Collaboration. An indication of anisotropy in arrival directions of ultra-high-energy cosmic rays through comparison to the flux pattern of extragalactic gamma-ray sources. *The Astrophysical Journal Letters*, 853(2):L29, 2018.
- [33] Cainã de Oliveira and Vitor de Souza. Magnetically induced anisotropies in the arrival directions of ultra-high-energy cosmic rays from nearby radio galaxies. *The Astrophysical Journal*, 925(1):42, jan 2022. doi: 10.3847/1538-4357/ac3753. URL <https://doi.org/10.3847/1538-4357/ac3753>.
- [34] The Telescope Array Collaboration. Indications of intermediate-scale anisotropy of cosmic rays with energy greater than 57 EeV in the northern sky measured with the surface detector of the Telescope Array Experiment. *The Astrophysical Journal*, 790(2):L21, jul 2014. doi: 10.1088/2041-8205/790/2/L21. URL <https://doi.org/10.1088/2041-8205/790/2/L21>.
- [35] Gustavo E. Romero, Jorge A. Combi, Santiago E. Perez Bergliffa, and Luis A. Anchordoqui. Centaurus A as a source of extragalactic cosmic rays with arrival energies well beyond the GZK cutoff. *Astroparticle Physics*, 5(3):279–283, 1996. ISSN 0927-6505. doi: [https://doi.org/10.1016/0927-6505\(96\)00029-1](https://doi.org/10.1016/0927-6505(96)00029-1). URL <https://www.sciencedirect.com/science/article/pii/0927650596000291>.

- [36] Peter L Biermann and Vitor De Souza. Centaurus A: The extragalactic source of cosmic rays with energies above the knee. *The Astrophysical Journal*, 746(1):72, 2012.
- [37] Ruo-Yu Liu, Xiang-Yu Wang, Wei Wang, and Andrew M Taylor. On the excess of ultra-high energy cosmic rays in the direction of Centaurus A. *The Astrophysical Journal*, 755(2):139, 2012.
- [38] Sarka Wykes, Judith H Croston, Martin J Hardcastle, Jean A Eilek, Peter L Biermann, Abraham Achterberg, Justin D Bray, Alex Lazarian, Marijke Haverkorn, Ray J Protheroe, et al. Mass entrainment and turbulence-driven acceleration of ultra-high energy cosmic rays in Centaurus A. *Astronomy & Astrophysics*, 558:A19, 2013.
- [39] Glennys R Farrar, Ronnie Jansson, Ilana J Feain, and B.M Gaensler. Galactic magnetic deflections and Centaurus A as a UHECR source. *Journal of Cosmology and Astroparticle Physics*, 2013(01):023–023, jan 2013. doi: 10.1088/1475-7516/2013/01/023. URL <https://doi.org/10.1088/1475-7516/2013/01/023>.
- [40] Sarka Wykes, Andrew M Taylor, Justin D Bray, Martin J Hardcastle, and Michael Hillas. UHECR propagation from Centaurus A. *Nuclear and particle physics proceedings*, 297:234–241, 2018.
- [41] Cainã de Oliveira and Vitor de Souza. Probing UHECR production in Centaurus A using secondary neutrinos and gamma-rays. *The European Physical Journal C*, 81(6):1–17, 2021.
- [42] Lorenzo Caccianiga. Anisotropies of the highest energy cosmic-ray events recorded by the Pierre Auger Observatory in 15 years of operation. In *36th International Cosmic Ray Conference*, volume 358, page 206. SISSA Medialab, 2019.
- [43] K Dolag, M Kachelrieß, and D.V Semikoz. UHECR observations and lensing in the magnetic field of the Virgo cluster. *Journal of Cosmology and Astroparticle Physics*, 2009(01):033–033, jan 2009. doi: 10.1088/1475-7516/2009/01/033. URL <https://doi.org/10.1088/1475-7516/2009/01/033>.
- [44] R. U. Abbasi, M. Abe, T. Abu-Zayyad, M. Allen, R. Azuma, E. Barcikowski, J. W. Belz, D. R. Bergman, S. A. Blake, R. Cady, B. G. Cheon, J. Chiba, M. Chikawa, A. di Matteo, T. Fujii, K. Fujita, M. Fukushima, G. Furlich, T. Goto, W. Hanlon, M. Hayashi, Y. Hayashi, N. Hayashida, K. Hibino, K. Honda, D. Ikeda, N. Inoue, T. Ishii, R. Ishimori, H. Ito, D. Ivanov, H. M. Jeong, S. Jeong, C. C. H. Jui, K. Kadota, F. Kakimoto, O. Kalashev, K. Kasahara, H. Kawai, S. Kawakami, S. Kawana, K. Kawata, E. Kido, H. B. Kim, J. H. Kim, J. H. Kim, S. Kishigami, S. Kitamura, Y. Kitamura, V. Kuzmin, M. Kuznetsov, Y. J. Kwon, K. H. Lee, B. Lubsandorzhev, J. P. Lundquist, K. Machida, K. Martens, T. Matsuyama, J. N. Matthews, R. Mayta, M. Minamino, K. Mukai, I. Myers, K. Nagasawa, S. Nagataki, R. Nakamura, T. Nakamura, T. Nonaka, H. Oda, S. Ogio, J. Ogura, M. Ohnishi, H. Ohoka, T. Okuda, Y. Omura, M. Ono, R. Onogi, A. Oshima, S. Ozawa, I. H. Park, M. S. Pshirkov, J. Remington, D. C. Rodriguez, G. Rubtsov, D. Ryu, H. Sagawa, R. Sahara, K. Saito, Y. Saito, N. Sakaki, N. Sakurai, L. M. Scott, T. Seki, K. Sekino, P. D. Shah, F. Shibata, T. Shibata, H. Shimodaira, B. K. Shin, H. S. Shin, J. D. Smith, P. Sokolsky, B. T. Stokes, S. R. Stratton, T. A. Stroman, T. Suzawa, Y. Takagi, Y. Takahashi, M. Takamura, M. Takeda, R. Takeishi, A. Taketa, M. Takita, Y. Tameda, H. Tanaka, K. Tanaka, M. Tanaka, S. B. Thomas, G. B. Thomson, P. Tinyakov, I. Tkachev, H. Tokuno, T. Tomida, S. Troitsky, Y. Tsunesada, K. Tsutsumi, Y. Uchihori, S. Udo, F. Urban, T. Wong, M. Yamamoto, R. Yamane, H. Yamaoka, K. Yamazaki, J. Yang, K. Yashiro, Y. Yoneda, S. Yoshida, H. Yoshii, Y. Zhezher, and Z. Zundel. Testing a reported correlation between arrival directions of ultra-high-energy cosmic rays and a flux pattern from nearby starburst galaxies using telescope array data. *The Astrophysical Journal*, 867(2):L27, nov 2018. doi: 10.3847/2041-8213/aabf9. URL <https://doi.org/10.3847/2041-8213/aabf9>.
- [45] M. Erdmann, G. Müller, M. Urban, and M. Wirtz. The nuclear window to the extragalactic

- universe. *Astroparticle Physics*, 85:54–64, 2016. ISSN 0927-6505. doi: <https://doi.org/10.1016/j.astropartphys.2016.10.002>. URL <https://www.sciencedirect.com/science/article/pii/S0927650516301451>.
- [46] Glennys R. Farrar and Michael S. Sutherland. Deflections of UHECRs in the galactic magnetic field. *Journal of Cosmology and Astroparticle Physics*, 2019(05):004–004, may 2019. doi: 10.1088/1475-7516/2019/05/004. URL <https://doi.org/10.1088/1475-7516/2019/05/004>.
- [47] Guenter Sigl, Francesco Miniati, and Torsten Ensslin. Signatures of magnetized large scale structure in ultra-high energy cosmic rays, 2003. URL <https://arxiv.org/abs/astro-ph/0309695>.
- [48] Günter Sigl, Francesco Miniati, and Torsten A. Ensslin. Ultrahigh energy cosmic rays in a structured and magnetized universe. *Phys. Rev. D*, 68:043002, Aug 2003. doi: 10.1103/PhysRevD.68.043002. URL <https://link.aps.org/doi/10.1103/PhysRevD.68.043002>.
- [49] Klaus Dolag, Dario Grasso, Volker Springel, and Igor Tkachev. Constrained simulations of the magnetic field in the local universe and the propagation of ultrahigh energy cosmic rays. *Journal of Cosmology and Astroparticle Physics*, 2005(01):009–009, jan 2005. doi: 10.1088/1475-7516/2005/01/009. URL <https://doi.org/10.1088/1475-7516/2005/01/009>.
- [50] Rafael Alves Batista, Min-Su Shin, Julien Devriendt, Dmitri Semikoz, and Guenter Sigl. Implications of strong intergalactic magnetic fields for ultrahigh-energy cosmic-ray astronomy. *Phys. Rev. D*, 96:023010, Jul 2017. doi: 10.1103/PhysRevD.96.023010. URL <https://link.aps.org/doi/10.1103/PhysRevD.96.023010>.
- [51] Kandaswamy Subramanian. The origin, evolution and signatures of primordial magnetic fields. *Reports on Progress in Physics*, 79(7):076901, may 2016. doi: 10.1088/0034-4885/79/7/076901. URL <https://doi.org/10.1088/0034-4885/79/7/076901>.
- [52] Stefan Hackstein, Franco Vazza, Marcus Brüggen, Jenny G Sorce, and Stefan Gottlöber. Simulations of ultra-high energy cosmic rays in the local universe and the origin of cosmic magnetic fields. *Monthly Notices of the Royal Astronomical Society*, 475(2):2519–2529, 2018.
- [53] Sun, X. H., Reich, W., Waelkens, A., and Enklin, T. A. Radio observational constraints on galactic 3d-emission models. *A&A*, 477(2):573–592, 2008. doi: 10.1051/0004-6361:20078671. URL <https://doi.org/10.1051/0004-6361:20078671>.
- [54] Ronnie Jansson and Glennys R. Farrar. A new model of the Galactic magnetic field. *The Astrophysical Journal*, 757(1):14, Aug 2012. ISSN 1538-4357. doi: 10.1088/0004-637x/757/1/14. URL <http://dx.doi.org/10.1088/0004-637X/757/1/14>.
- [55] Ronnie Jansson and Glennys R. Farrar. The Galactic Magnetic Field. *The Astrophysical Journal*, 761(1):L11, nov 2012. doi: 10.1088/2041-8205/761/1/L11. URL <https://doi.org/10.1088/2041-8205/761/1/L11>.
- [56] M. S. Pshirkov, P. G. Tinyakov, P. P. Kronberg, and K. J. Newton-McGee. DERIVING THE GLOBAL STRUCTURE OF THE GALACTIC MAGNETIC FIELD FROM FARADAY ROTATION MEASURES OF EXTRAGALACTIC SOURCES. *The Astrophysical Journal*, 738(2):192, aug 2011. doi: 10.1088/0004-637x/738/2/192. URL <https://doi.org/10.1088/0004-637x/738/2/192>.
- [57] Georgi T Zatspein and Vadem A Kuz'min. Upper limit of the spectrum of cosmic rays. *Soviet Journal of Experimental and Theoretical Physics Letters*, 4:78, 1966.
- [58] Kenneth Greisen. End to the cosmic-ray spectrum? *Phys. Rev. Lett.*, 16(17):748–, April 1966. URL <http://link.aps.org/abstract/PRL/v16/p748>.
- [59] Olivier Deligny, Antoine Letessier-Selvon, and Etienne Parizot. Magnetic horizons of uhedr sources and the gzk feature. *Astroparticle Physics*, 21(6):609–615, 2004. ISSN 0927-6505. doi:

<https://doi.org/10.1016/j.astropartphys.2004.04.012>. URL
<https://www.sciencedirect.com/science/article/pii/S0927650504000908>.

- [60] Andrew M Taylor, Markus Ahlers, and Felix A Aharonian. Need for a local source of ultrahigh-energy cosmic-ray nuclei. *Physical Review D*, 84(10):105007, 2011.
- [61] Rafael Alves Batista and Günter Sigl. Magnetic horizons of ultra-high energy cosmic rays. In *20th International Conference on Particles and Nuclei*, pages 387–390, 9 2014. doi: 10.3204/DESY-PROC-2014-04/127.
- [62] Rodrigo Guedes Lang, Andrew M Taylor, Markus Ahlers, and Vitor de Souza. Revisiting the distance to the nearest ultrahigh energy cosmic ray source: Effects of extragalactic magnetic fields. *Physical Review D*, 102(6):063012, 2020.
- [63] Rodrigo Guedes Lang, Andrew M. Taylor, and Vitor de Souza. Ultrahigh-energy cosmic rays dipole and beyond. *Phys. Rev. D*, 103:063005, Mar 2021. doi: 10.1103/PhysRevD.103.063005. URL <https://link.aps.org/doi/10.1103/PhysRevD.103.063005>.
- [64] James W. Cronin. Cosmic rays: the most energetic particles in the universe. *Rev. Mod. Phys.*, 71:S165–S172, Mar 1999. doi: 10.1103/RevModPhys.71.S165. URL <https://link.aps.org/doi/10.1103/RevModPhys.71.S165>.
- [65] Alberto Daniel Supanitsky and V de Souza. An upper limit on the cosmic-ray luminosity of individual sources from gamma-ray observations. *Journal of Cosmology and Astroparticle Physics*, 2013(12):023, 2013.
- [66] Kumiko Kotera and Angela V Olinto. The astrophysics of ultrahigh-energy cosmic rays. *Annual Review of Astronomy and Astrophysics*, 49:119–153, 2011.
- [67] A. Aab, P. Abreu, M. Aglietta, J. M. Albury, I. Allekotte, A. Almela, J. Alvarez Castillo, J. Alvarez-Muñiz, R. Alves Batista, G. A. Anastasi, L. Anchordoqui, B. Andrada, S. Andringa, C. Aramo, P. R. Araújo Ferreira, H. Asorey, P. Assis, G. Avila, A. M. Badescu, A. Bakalova, A. Balaceanu, F. Barbato, R. J. Barreira Luz, K. H. Becker, J. A. Bellido, C. Berat, M. E. Bertaina, X. Bertou, P. L. Biermann, T. Bister, J. Biteau, A. Blanco, J. Blazek, C. Bleve, M. Boháčová, D. Boncioli, C. Bonifazi, L. Bonneau Arbetletche, N. Borodai, A. M. Botti, J. Brack, T. Bretz, F. L. Briechle, P. Buchholz, A. Bueno, S. Buitink, M. Buscemi, K. S. Caballero-Mora, L. Caccianiga, L. Calcagni, A. Cancio, F. Canfora, I. Caracas, J. M. Carceller, R. Caruso, A. Castellina, F. Catalani, G. Cataldi, L. Cazon, M. Cerda, J. A. Chinellato, K. Choi, J. Chudoba, L. Chytka, R. W. Clay, A. C. Cobos Cerutti, R. Colalillo, A. Coleman, M. R. Coluccia, R. Conceição, A. Condorelli, G. Consolati, F. Contreras, F. Convenga, C. E. Covault, S. Dasso, K. Daumiller, B. R. Dawson, J. A. Day, R. M. de Almeida, J. de Jesús, S. J. de Jong, G. De Mauro, J. R. T. de Mello Neto, I. De Mitri, J. de Oliveira, D. de Oliveira Franco, V. de Souza, E. De Vito, J. Debatin, M. del Río, O. Deligny, H. Dembinski, N. Dhital, C. Di Giulio, A. Di Matteo, M. L. Díaz Castro, C. Dobrigkeit, J. C. D’Olivo, Q. Dorosti, R. C. dos Anjos, M. T. Dova, J. Ebr, R. Engel, I. Epicoco, M. Erdmann, C. O. Escobar, A. Etchegoyen, H. Falcke, J. Farmer, G. Farrar, A. C. Fauth, N. Fazzini, F. Feldbusch, F. Fenu, B. Fick, J. M. Figueira, A. Filipčič, T. Fodran, M. M. Freire, T. Fujii, A. Fuster, C. Galea, C. Galelli, B. García, A. L. Garcia Vegas, H. Gemmeke, F. Gesualdi, A. Gherghel-Lascu, P. L. Ghia, U. Giaccari, M. Giammarchi, M. Giller, J. Glombitza, F. Gobbi, F. Gollan, G. Golup, M. Gómez Berisso, P. F. Gómez Vitale, J. P. Gongora, N. González, I. Goos, D. Góra, A. Gorgi, M. Gottowik, T. D. Grubb, F. Guarino, G. P. Guedes, E. Guido, S. Hahn, R. Halliday, M. R. Hampel, P. Hansen, D. Harari, V. M. Harvey, A. Haungs, T. Hebbeker, D. Heck, G. C. Hill, C. Hojvat, J. R. Hörandel, P. Horvath, M. Hrabovský, T. Huege, J. Hulsman, A. Insolia, P. G. Isar, J. A. Johnsen, J. Jurysek, A. Kääpä, K. H. Kampert, B. Keilhauer, J. Kemp, H. O. Klages, M. Kleifges, J. Kleinfeller, M. Köpke, G. Kukec Mezek, B. L. Lago, D. LaHurd, R. G. Lang, M. A. Leigui de Oliveira, V. Lenok, A. Letessier-Selvon, I. Lhenry-Yvon, D. Lo Presti, L. Lopes, R. López, R. Lorek, Q. Luce, A. Lucero, A. Machado Payeras, M. Malacari, G. Mancarella, D. Mandat, B. C.

Manning, J. Manshanden, P. Mantsch, S. Marafico, A. G. Mariazzi, I. C. Mariş, G. Marsella, D. Martello, H. Martinez, O. Martínez Bravo, M. Mastrodicasa, H. J. Mathes, J. Matthews, G. Matthiae, E. Mayotte, P. O. Mazur, G. Medina-Tanco, D. Melo, A. Menshikov, K.-D. Merenda, S. Michal, M. I. Micheletti, L. Miramonti, D. Mockler, S. Mollerach, F. Montanet, C. Morello, M. Mostafá, A. L. Müller, M. A. Muller, K. Mulrey, R. Mussa, M. Muzio, W. M. Namasaka, L. Nellen, P. H. Nguyen, M. Niculescu-Oglinzanu, M. Niechciol, D. Nitz, D. Nosek, V. Novotny, L. Nožka, A. Nucita, L. A. Núñez, M. Palatka, J. Pallotta, M. P. Panetta, P. Papenbreer, G. Parente, A. Parra, M. Pech, F. Pedreira, J. Pękala, R. Pelayo, J. Peña Rodriguez, J. Perez Armand, M. Perlin, L. Perrone, C. Peters, S. Petrera, T. Pierog, M. Pimenta, V. Pirronello, M. Platino, B. Pont, M. Pothast, P. Privitera, M. Prouza, A. Puyleart, S. Querschfeld, J. Rautenberg, D. Ravignani, M. Reininghaus, J. Ridky, F. Riehn, M. Risse, P. Ristori, V. Rizi, W. Rodrigues de Carvalho, G. Rodriguez Fernandez, J. Rodriguez Rojo, M. J. Roncoroni, M. Roth, E. Roulet, A. C. Rovero, P. Ruehl, S. J. Saffi, A. Saftoiu, F. Salamida, H. Salazar, G. Salina, J. D. Sanabria Gomez, F. Sánchez, E. M. Santos, E. Santos, F. Sarazin, R. Sarmiento, C. Sarmiento-Cano, R. Sato, P. Savina, C. Schäfer, V. Scherini, H. Schieler, M. Schimassek, M. Schimp, F. Schlüter, D. Schmidt, O. Scholten, P. Schovánek, F. G. Schröder, S. Schröder, A. Schulz, S. J. Sciutto, M. Scornavacche, R. C. Shellard, G. Sigl, G. Silli, O. Sima, R. Šmída, P. Sommers, J. F. Soriano, J. Souchard, R. Squartini, M. Stadelmaier, D. Stanca, S. Stanič, J. Stasielak, P. Stassi, A. Streich, M. Suárez-Durán, T. Sudholz, T. Suomijärvi, A. D. Supanitsky, J. Šupík, Z. Szadkowski, A. Taboada, A. Tapia, C. Timmermans, O. Tkachenko, P. Tobiska, C. J. Todero Peixoto, B. Tomé, G. Torralba Elipe, A. Travaini, P. Travnicek, C. Trimarelli, M. Trini, M. Tueros, R. Ulrich, M. Unger, M. Urban, L. Vaclavek, M. Vacula, J. F. Valdés Galicia, I. Valiño, L. Valore, A. van Vliet, E. Varela, B. Vargas Cárdenas, A. Vásquez-Ramírez, D. Veberič, C. Ventura, I. D. Vergara Quispe, V. Verzi, J. Vicha, L. Villaseñor, J. Vink, S. Vorobiov, H. Wahlberg, A. A. Watson, M. Weber, A. Weindl, L. Wiencke, H. Wilczyński, T. Winchen, M. Wirtz, D. Wittkowski, B. Wundheiler, A. Yushkov, O. Zapparrata, E. Zas, D. Zavrtanik, M. Zavrtanik, L. Zehrer, A. Zepeda, M. Ziolkowski, and F. Zuccarello. Measurement of the cosmic-ray energy spectrum above 2.5×10^{18} eV using the Pierre Auger Observatory. *Phys. Rev. D*, 102:062005, Sep 2020. doi: 10.1103/PhysRevD.102.062005. URL <https://link.aps.org/doi/10.1103/PhysRevD.102.062005>.

- [68] M. Ackermann, M. Ajello, A. Allafort, L. Baldini, J. Ballet, D. Bastieri, K. Bechtol, R. Bellazzini, B. Berenji, E. D. Bloom, E. Bonamente, A. W. Borgland, A. Bouvier, J. Bregeon, M. Brigida, P. Bruel, R. Buehler, S. Buson, G. A. Caliandro, R. A. Cameron, P. A. Caraveo, J. M. Casandjian, C. Cecchi, E. Charles, A. Chekhtman, C. C. Cheung, J. Chiang, A. N. Cillis, S. Ciprini, R. Claus, J. Cohen-Tanugi, J. Conrad, S. Cutini, F. de Palma, C. D. Dermer, S. W. Digel, E. do Couto e Silva, P. S. Drell, A. Drlica-Wagner, C. Favuzzi, S. J. Fegan, P. Fortin, Y. Fukazawa, S. Funk, P. Fusco, F. Gargano, D. Gasparrini, S. Germani, N. Giglietto, F. Giordano, T. Glanzman, G. Godfrey, I. A. Grenier, S. Guiriec, M. Gustafsson, D. Hadasch, M. Hayashida, E. Hays, R. E. Hughes, G. Jóhannesson, A. S. Johnson, T. Kamae, H. Katagiri, J. Kataoka, J. Knödlseider, M. Kuss, J. Lande, F. Longo, F. Loparco, B. Lott, M. N. Lovellette, P. Lubrano, G. M. Madejski, P. Martin, M. N. Mazziotta, J. E. McEnery, P. F. Michelson, T. Mizuno, C. Monte, M. E. Monzani, A. Morselli, I. V. Moskalenko, S. Murgia, S. Nishino, J. P. Norris, E. Nuss, M. Ohno, T. Ohsugi, A. Okumura, N. Omodei, E. Orlando, M. Ozaki, D. Parent, M. Persic, M. Pesce-Rollins, V. Petrosian, M. Pierbattista, F. Piron, G. Pivato, T. A. Porter, S. Rainò, R. Rando, M. Razzano, A. Reimer, O. Reimer, S. Ritz, M. Roth, C. Sbarra, C. Sgrò, E. J. Siskind, G. Spandre, P. Spinelli, Łukasz Stawarz, A. W. Strong, H. Takahashi, T. Tanaka, J. B. Thayer, L. Tibaldo, M. Tinivella, D. F. Torres, G. Tosti, E. Troja, Y. Uchiyama, J. Vandenbroucke, G. Vianello, V. Vitale, A. P. Waite, M. Wood, and Z. Yang. GeV OBSERVATIONS OF STAR-FORMING GALAXIES WITH THE *FERMI* LARGE AREA TELESCOPE. *The Astrophysical Journal*, 755(2):164, aug 2012. doi: 10.1088/0004-637x/755/2/164. URL <https://doi.org/10.1088/0004-637x/755/2/164>.

- [69] Sahakyan, N., Baghmanyany, V., and Zargaryan, D. Fermi-lat observation of nonblazar agns. *A&A*, 614:A6, 2018. doi: 10.1051/0004-6361/201732304. URL <https://doi.org/10.1051/0004-6361/201732304>.
- [70] Rafael Alves Batista, Andrej Dundovic, Martin Erdmann, Karl-Heinz Kampert, Daniel Kuempel, Gero Müller, Guenter Sigl, Arjen van Vliet, David Walz, and Tobias Winchen. CRPropa 3 – a public astrophysical simulation framework for propagating extraterrestrial ultra-high energy particles. *Journal of Cosmology and Astroparticle Physics*, 2016(05):038, 2016.
- [71] Rudy C Gilmore, Rachel S Somerville, Joel R Primack, and Alberto Domínguez. Semi-analytic modelling of the extragalactic background light and consequences for extragalactic gamma-ray spectra. *Monthly Notices of the Royal Astronomical Society*, 422(4):3189–3207, 2012.
- [72] Hans-Peter Bretz, Martin Erdmann, Peter Schiffer, David Walz, and Tobias Winchen. Parsec: A parametrized simulation engine for ultra-high energy cosmic ray protons. *Astroparticle Physics*, 54:110–117, 2014. ISSN 0927-6505. doi: <https://doi.org/10.1016/j.astropartphys.2013.12.002>. URL <https://www.sciencedirect.com/science/article/pii/S0927650513001874>.
- [73] Alessandra Lamastra, Fabrizio Tavecchio, Patrizia Romano, Marco Landoni, and Stefano Vercellone. Unveiling the origin of the gamma-ray emission in ngc 1068 with the cherenkov telescope array. *Astroparticle Physics*, 112:16–23, 2019. ISSN 0927-6505. doi: <https://doi.org/10.1016/j.astropartphys.2019.04.003>. URL <https://www.sciencedirect.com/science/article/pii/S0927650519300362>.
- [74] J Aublin and E Parizot. Generalised 3d-reconstruction method of a dipole anisotropy in cosmic-ray distributions. *Astronomy & Astrophysics*, 441(1):407–415, 2005.
- [75] Günter Sigl, Francesco Miniati, and Torsten A. Ensslin. Cosmic magnetic fields and their influence on ultra-high energy cosmic ray propagation. *Nuclear Physics B - Proceedings Supplements*, 136:224–233, 2004. ISSN 0920-5632. doi: <https://doi.org/10.1016/j.nuclphysbps.2004.10.043>. URL <https://www.sciencedirect.com/science/article/pii/S0920563204004608>. CRIS 2004 Proceedings of the Cosmic Ray International Seminars: GZK and Surroundings.
- [76] Gustavo Medina Tanco. *Cosmic Magnetic Fields from the Perspective of Ultra-High-Energy Cosmic Rays Propagation*, pages 155–180. Springer Berlin Heidelberg, Berlin, Heidelberg, 2001. ISBN 978-3-540-45615-5. doi: 10.1007/3-540-45615-5_7. URL https://doi.org/10.1007/3-540-45615-5_7.
- [77] Gustavo A. Medina Tanco. The effect of highly structured cosmic magnetic fields on ultra-high-energy cosmic-ray propagation. *The Astrophysical Journal*, 505(2):L79–L82, oct 1998. doi: 10.1086/311615. URL <https://doi.org/10.1086/311615>.
- [78] Sangjin Lee, Angela V. Olinto, and Guenter Sigl. Extragalactic Magnetic Field and the Highest Energy Cosmic Rays. *The Astrophysical Journal Letter*, 455:L21, December 1995. doi: 10.1086/309812.
- [79] A. Aab, P. Abreu, M. Aglietta, I. Al Samarai, I. F. M. Albuquerque, I. Allekotte, A. Almela, J. Alvarez Castillo, J. Alvarez-Muñiz, G. A. Anastasi, L. Anchordoqui, B. Andrada, S. Andringa, C. Aramo, F. Arqueros, N. Arsene, H. Asorey, P. Assis, J. Aublin, G. Avila, A. M. Badescu, A. Balaceanu, F. Barbato, R. J. Barreira Luz, J. J. Beatty, K. H. Becker, J. A. Bellido, C. Berat, M. E. Bertaina, X. Bertou, P. L. Biermann, J. Biteau, S. G. Blaess, A. Blanco, J. Blazek, C. Bleve, M. Boháčová, D. Boncioli, C. Bonifazi, N. Borodai, A. M. Botti, J. Brack, I. Brancus, T. Bretz, A. Bridgeman, F. L. Briechle, P. Buchholz, A. Bueno, S. Buitink, M. Buscemi, K. S. Caballero-Mora, L. Caccianiga, A. Cancio, F. Canfora, L. Caramete, R. Caruso, A. Castellina, F. Catalani, G. Cataldi, L. Cazon, A. G. Chavez, J. A. Chinellato, J. Chudoba, R. W. Clay, A. Cobos, R. Colalillo, A. Coleman, L. Collica, M. R.

Coluccia, R. Conceição, G. Consolati, F. Contreras, M. J. Cooper, S. Coutu, C. E. Covault, J. Cronin, S. D'Amico, B. Daniel, S. Dasso, K. Daumiller, B. R. Dawson, R. M. de Almeida, S. J. de Jong, G. De Mauro, J. R. T. de Mello Neto, I. De Mitri, J. de Oliveira, V. de Souza, J. Debatin, O. Deligny, M. L. Díaz Castro, F. Diogo, C. Dobrigkeit, J. C. D'Olivo, Q. Dorosti, R. C. dos Anjos, M. T. Dova, A. Dundovic, J. Ebr, R. Engel, M. Erdmann, M. Erfani, C. O. Escobar, J. Espadanal, A. Etchegoyen, H. Falcke, J. Farmer, G. Farrar, A. C. Fauth, N. Fazzini, F. Fenu, B. Fick, J. M. Figueira, A. Filipčič, O. Fratu, M. M. Freire, T. Fujii, A. Fuster, R. Gaior, B. García, D. Garcia-Pinto, F. Gaté, H. Gemmeke, A. Gherghel-Lascu, P. L. Ghia, U. Giaccari, M. Giammarchi, M. Giller, D. Głás, C. Glaser, G. Golup, M. Gómez Berisso, P. F. Gómez Vitale, N. González, A. Gorgi, P. Gorham, A. F. Grillo, T. D. Grubb, F. Guarino, G. P. Guedes, R. Halliday, M. R. Hampel, P. Hansen, D. Harari, T. A. Harrison, J. L. Harton, A. Haungs, T. Hebbeker, D. Heck, P. Heimann, A. E. Herve, G. C. Hill, C. Hojvat, E. Holt, P. Homola, J. R. Hörandel, P. Horvath, M. Hrabovský, T. Huege, J. Hulsman, A. Insolia, P. G. Isar, I. Jandt, J. A. Johnsen, M. Josebachuili, J. Jurysek, A. Kääpä, O. Kambeitz, K. H. Kampert, B. Keilhauer, N. Kemmerich, E. Kemp, J. Kemp, R. M. Kieckhafer, H. O. Klages, M. Kleifges, J. Kleinfeller, R. Krause, N. Krohm, D. Kuempel, G. Kukec Mezek, N. Kunka, A. Kuotb Awad, B. L. Lago, D. LaHurd, R. G. Lang, M. Lauscher, R. Legumina, M. A. Leigui de Oliveira, A. Letessier-Selvon, I. Lhenry-Yvon, K. Link, D. Lo Presti, L. Lopes, R. López, A. López Casado, R. Lorek, Q. Luce, A. Lucero, M. Malacari, M. Mallamaci, D. Mandat, P. Mantsch, A. G. Mariazzi, I. C. Mariş, G. Marsella, D. Martello, H. Martinez, O. Martínez Bravo, J. J. Masías Meza, H. J. Mathes, S. Mathys, J. Matthews, J. A. J. Matthews, G. Matthiae, E. Mayotte, P. O. Mazur, C. Medina, G. Medina-Tanco, D. Melo, A. Menshikov, K.-D. Merenda, S. Michal, M. I. Micheletti, L. Middendorf, L. Miramonti, B. Mitrica, D. Mockler, S. Mollerach, F. Montanet, C. Morello, M. Mostafá, A. L. Müller, G. Müller, M. A. Muller, S. Müller, R. Mussa, I. Naranjo, L. Nellen, P. H. Nguyen, M. Niculescu-Oglinzanu, M. Niechciol, L. Niemietz, T. Niggemann, D. Nitz, D. Nosek, V. Novotny, L. Nožka, L. A. Núñez, L. Ochilo, F. Oikonomou, A. Olinto, M. Palatka, J. Pallotta, P. Papenbreer, G. Parente, A. Parra, T. Paul, M. Pech, F. Pedreira, J. Pękala, R. Pelayo, J. Peña Rodriguez, L. A. S. Pereira, M. Perlin, L. Perrone, C. Peters, S. Petrer, J. Phuntsok, R. Piegai, T. Pierog, M. Pimenta, V. Pirronello, M. Platino, M. Plum, C. Porowski, R. R. Prado, P. Privitera, M. Prouza, E. J. Quel, S. Quercfeld, S. Quinn, R. Ramos-Pollan, J. Rautenberg, D. Ravignani, J. Ridky, F. Riehn, M. Risse, P. Ristori, V. Rizi, W. Rodrigues de Carvalho, G. Rodriguez Fernandez, J. Rodriguez Rojo, D. Rogozin, M. J. Roncoroni, M. Roth, E. Roulet, A. C. Rovero, P. Ruehl, S. J. Saffi, A. Saftoiu, F. Salamida, H. Salazar, A. Saleh, F. Salesa Greus, G. Salina, F. Sánchez, P. Sanchez-Lucas, E. M. Santos, E. Santos, F. Sarazin, R. Sarmento, C. Sarmiento-Cano, R. Sato, M. Schauer, V. Scherini, H. Schieler, M. Schimp, D. Schmidt, O. Scholten, P. Schovánek, F. G. Schröder, S. Schröder, A. Schulz, J. Schumacher, S. J. Sciutto, A. Segreto, A. Shadkam, R. C. Shellard, G. Sigl, G. Silli, O. Sima, A. Śmiałkowski, R. Šmída, B. Smith, G. R. Snow, P. Sommers, S. Sonntag, R. Squartini, D. Stanca, S. Stanič, J. Stasielak, P. Stassi, M. Stolpovskiy, F. Strafella, A. Streich, F. Suarez, M. Suarez Durán, T. Sudholz, T. Suomijärvi, A. D. Supanitsky, J. Šupík, J. Swain, Z. Szadkowski, A. Taboada, O. A. Taborda, V. M. Theodoro, C. Timmermans, C. J. Todero Peixoto, L. Tomankova, B. Tomé, G. Torralba Elipse, P. Travnicek, M. Trini, R. Ulrich, M. Unger, M. Urban, J. F. Valdés Galicia, I. Valiño, L. Valore, G. van Aar, P. van Bodegom, A. M. van den Berg, A. van Vliet, E. Varela, B. Vargas Cárdenas, G. Varner, R. A. Vázquez, D. Veberič, C. Ventura, I. D. Vergara Quispe, V. Verzi, J. Vicha, L. Villaseñor, S. Vorobiov, H. Wahlberg, O. Wainberg, D. Walz, A. A. Watson, M. Weber, A. Weindl, L. Wiencke, H. Wilczyński, C. Wileman, M. Wirtz, D. Wittkowski, B. Wundheiler, L. Yang, A. Yushkov, E. Zas, D. Zavrtnik, M. Zavrtnik, A. Zepeda, B. Zimmermann, M. Ziolkowski, Z. Zong, and F. Zuccarello. Inferences on mass composition and tests of hadronic interactions from 0.3 to 100 eev using the water-cherenkov detectors of the pierre auger observatory. *Phys. Rev. D*, 96:122003, Dec 2017. doi: 10.1103/PhysRevD.96.122003. URL

<https://link.aps.org/doi/10.1103/PhysRevD.96.122003>.

- [80] A. M. Hillas. Cosmic rays: Recent progress and some current questions, 2006. URL <https://arxiv.org/abs/astro-ph/0607109>.
- [81] C.J. Todero Peixoto, Vitor de Souza, and Peter L. Biermann. Cosmic rays: the spectrum and chemical composition from 10^{10} to 10^{20} eV. *Journal of Cosmology and Astroparticle Physics*, 2015(07):042–042, jul 2015. doi: 10.1088/1475-7516/2015/07/042. URL <https://doi.org/10.1088/1475-7516/2015/07/042>.
- [82] Bohdan Paczynski. Gamma-ray bursts as hypernovae. *Fourth Huntsville gamma-ray burst symposium. AIP Conference Proceedings*, 428, 1998.
- [83] Xiang-Yu Wang, Soebur Razzaque, and Peter Mészáros. On the origin and survival of ultra-high-energy cosmic-ray nuclei in gamma-ray bursts and hypernovae. *The Astrophysical Journal*, 677:432, 2008.
- [84] P. Blasi, R. I. Epstein, and A. V. Olinto. Ultra-high-energy cosmic rays from young neutron star winds. *The Astrophysical Journal*, 533(2):L123–L126, apr 2000. doi: 10.1086/312626. URL <https://doi.org/10.1086/312626>.
- [85] R. Aloisio, V. Berezhinsky, and P. Blasi. Ultra high energy cosmic rays: implications of auger data for source spectra and chemical composition. *Journal of Cosmology and Astroparticle Physics*, 2014(10):020, 2014. URL <http://stacks.iop.org/1475-7516/2014/i=10/a=020>.

A Effect of the GMF over the hotspots

To illustrate the effect of the GMF, we compare the arrival direction of UHECR with energies above 60 EeV in the presence and in the absence of the GMF. Figure 12 and 13 shows the arrival directions map for events with energies above 60 EeV when local AGNs and SBGs were considered the sources of UHECR, respectively. The GMF effect is not included in these sky maps. These figures are analogues to the figures 3 and 4, in which the effect of the GMF is included. Comparing the figures, the effect of the GMF over the regions with excess of events from one particular source can be observed. In all the cases, it is possible to note that the GMF is responsible for blur the signal, since the arrival direction in the absence of the GMF is much more point-like.

Comparing figures 12 and 3, we can obtain the effects causing in the AGN cases. In the absence of the GMF, the events coming from Cen A majority are inside the HS1 region. The GMF acts attracting the events of Cen A to lower latitudes, removing them from the HS1 region. The GMF tends to attract the Vir A signal to lower latitudes in the cases in which the EGMF causes a small deflection, and to increase the deflection in direction to the HS3 region in the case of a large shift due to the EGMF. Over the events coming from For A, the GMF attract them to higher latitude, contributing to the population of the HS2.

Comparing figures 13 and 4, we can obtain the effects causing in the SBG cases. The most pronounced effect is to blur the events of the majority of sources. The GMF act over the events of M83 attracting the light fraction inside the HS1 and blurring the heavier fraction. In addition, the GMF relocate the contribution of NGC 4945, pulling events from that source from the direction of HS1. The GMF is also the responsible for attract the events from NGC 253 to the direction of the HS2, forming a large strip coming from lower latitudes.

Table 1. Properties of the sources considered: source name, distance, the radio luminosity at 1.4 GHz (L_{radio}) and the γ -ray luminosity between 0.1 and 100 GeV (L_γ).

Source	Distance (Mpc)	L_{radio} (10^{38} erg s $^{-1}$)	L_γ (10^{40} erg s $^{-1}$)
NGC 253	2.7	1.0	0.8
M82	3.6	1.3	1.7
NGC 4945	4.0	1.0	1.4
M83	4.0	0.4	1.0
IC 342	4.0	0.5	0.4
NGC 6946	5.9	0.7	0.5
NGC 2903	6.6	0.7	0.9
NGC 5055	7.8	0.6	1.1
NGC 3628	8.1	1.0	1.8
NGC 3627	8.1	0.7	2.0
NGC 4631	8.7	1.1	1.0
M51	10.3	1.2	2.9
NGC 891	11	0.9	4.4
NGC 3556	11.4	0.8	2.6
NGC 660	15	0.9	5.8
NGC 2146	16.3	4.1	15.4
NGC 3079	17.4	5.0	5.7
NGC 1068	17.9	17.8	17.7
NGC 1365	22.3	3.1	10.7
Centaurus A	3.8	260	11.2
Virgo A	18.4	760	78.9
Fornax A	20.9	830	27.8

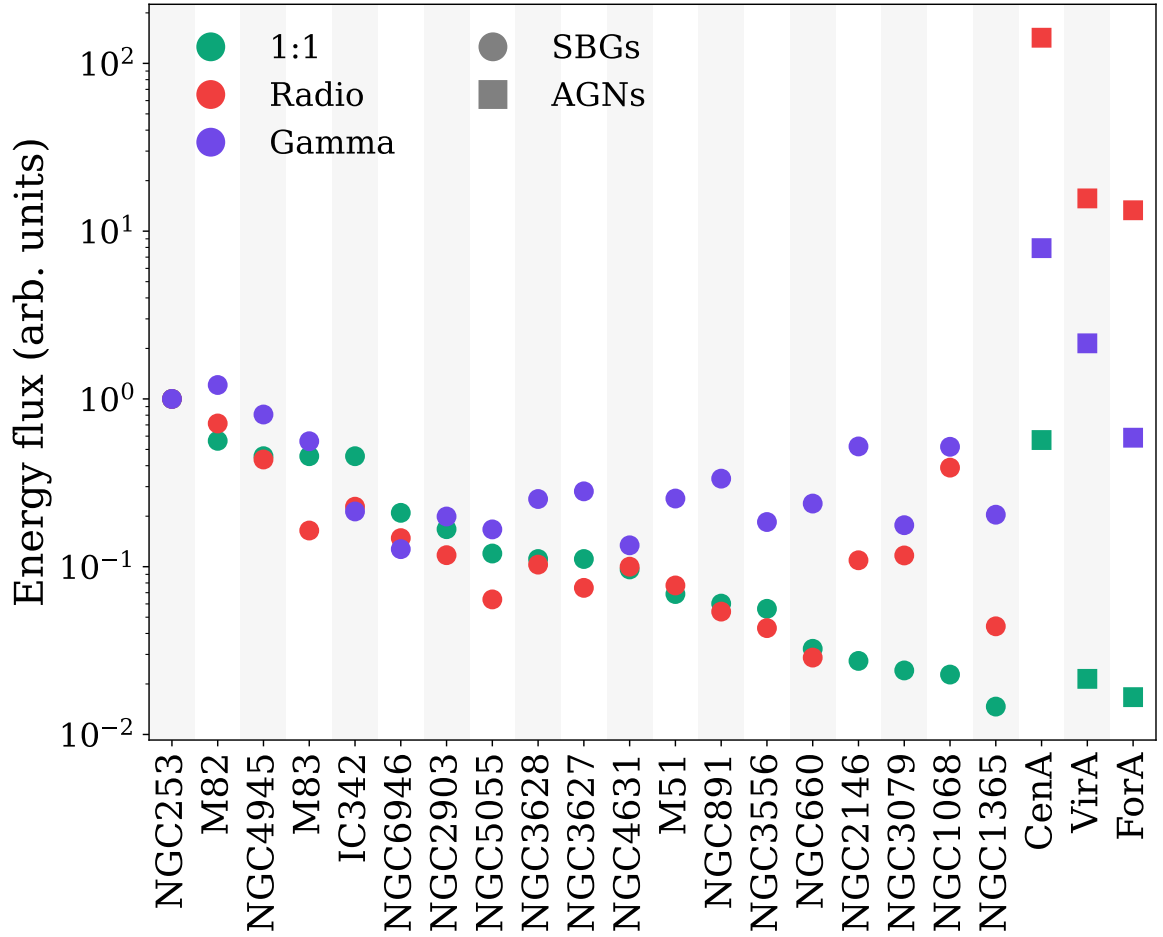


Figure 1. Energy flux at Earth from each source evaluated as L_{CR}/D^2 . Sources are plotted in order of distance from Earth inside its classification SBGs (circles) and AGNs (squares). NGC 253, the closest sources, has its flux arbitrarily set to one. Three proxies to the UHECR luminosity are presented (1:1, Radio, and Gamma).

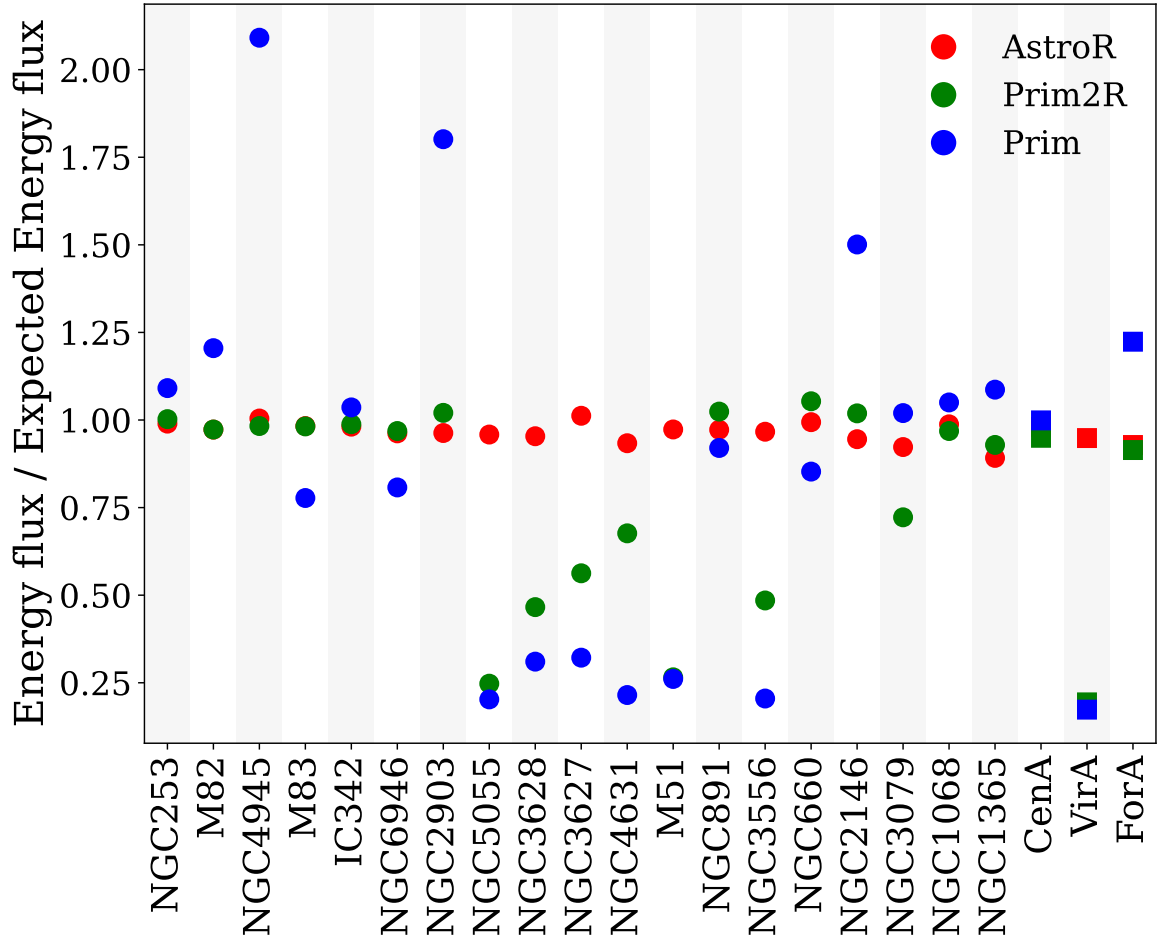


Figure 2. Ratio between the energy flux detected at Earth and the expected energy flux from the sources. Only protons emitted by the sources are considered. The EGMFs models AstroR (red), Prim2R (green), and Prim (blue) are shown. SBGs (circles) and AGNs (squares) are shown.

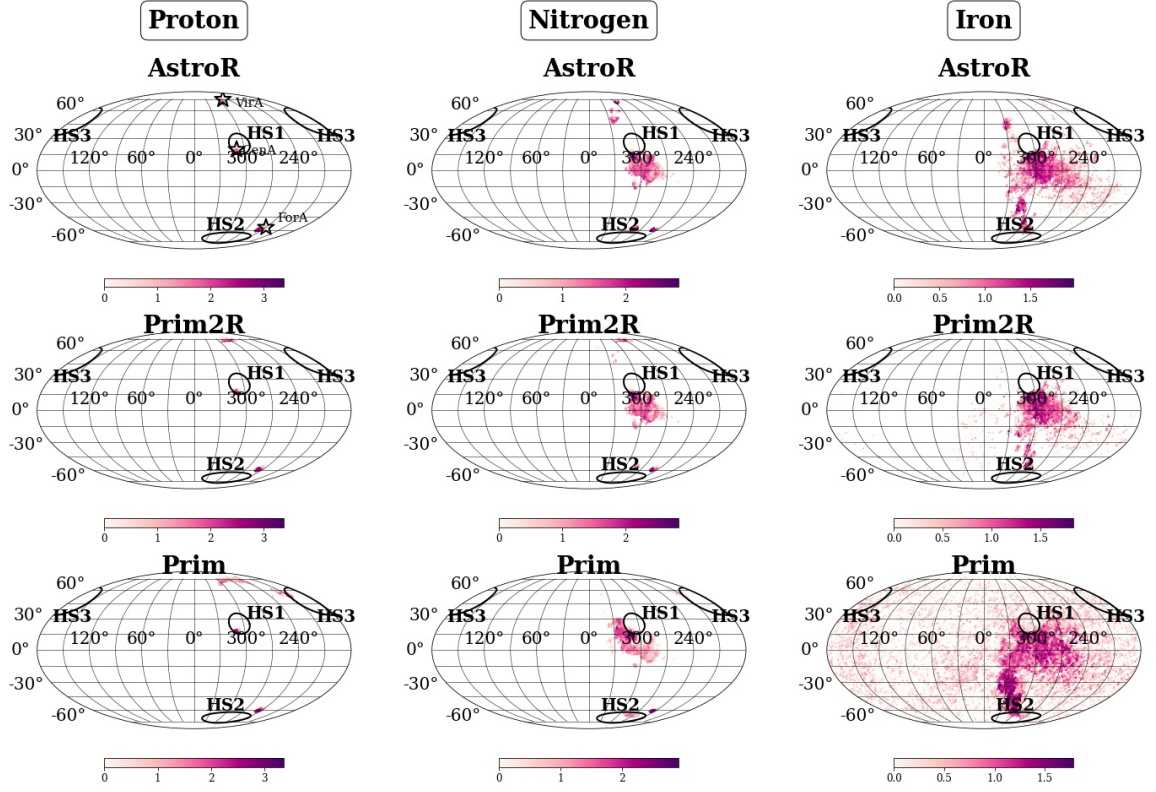


Figure 3. Arrival directions map (galactic coordinates) in a Mollweide projection for events with energies above 60 EeV arriving at Earth injected by the AGNs (Cen A, Vir A, and For A). The maps correspond to the 1:1 UHECR luminosity. The colorscale indicates the number of events on logarithm scale. In each line, an EGMF model is presented: AstroR, Prim2R, and Prim. In each column, the injected composition is shown: proton, nitrogen, and iron. The position of the sources (AGNs) is shown only in the first plot for sake of clarity. The hotspot regions measured by the Pierre Auger (HS1 and HS2) and the Telescope Array (HS3) are also shown.

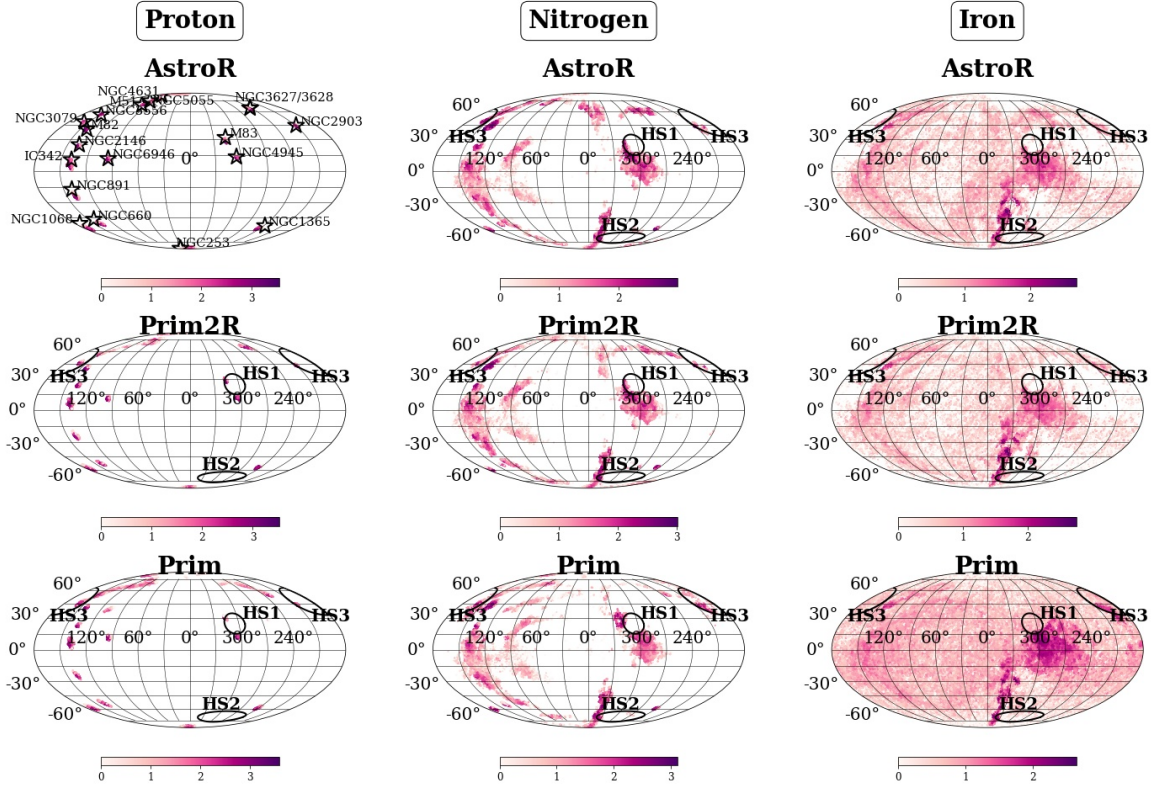


Figure 4. Arrival directions map in a Mollweide projection for events with energies above 60 EeV arriving at Earth injected by the SBGs in Table 1. The maps correspond to the 1:1 UHECR luminosity. The elements of figure are the same of figure 3.

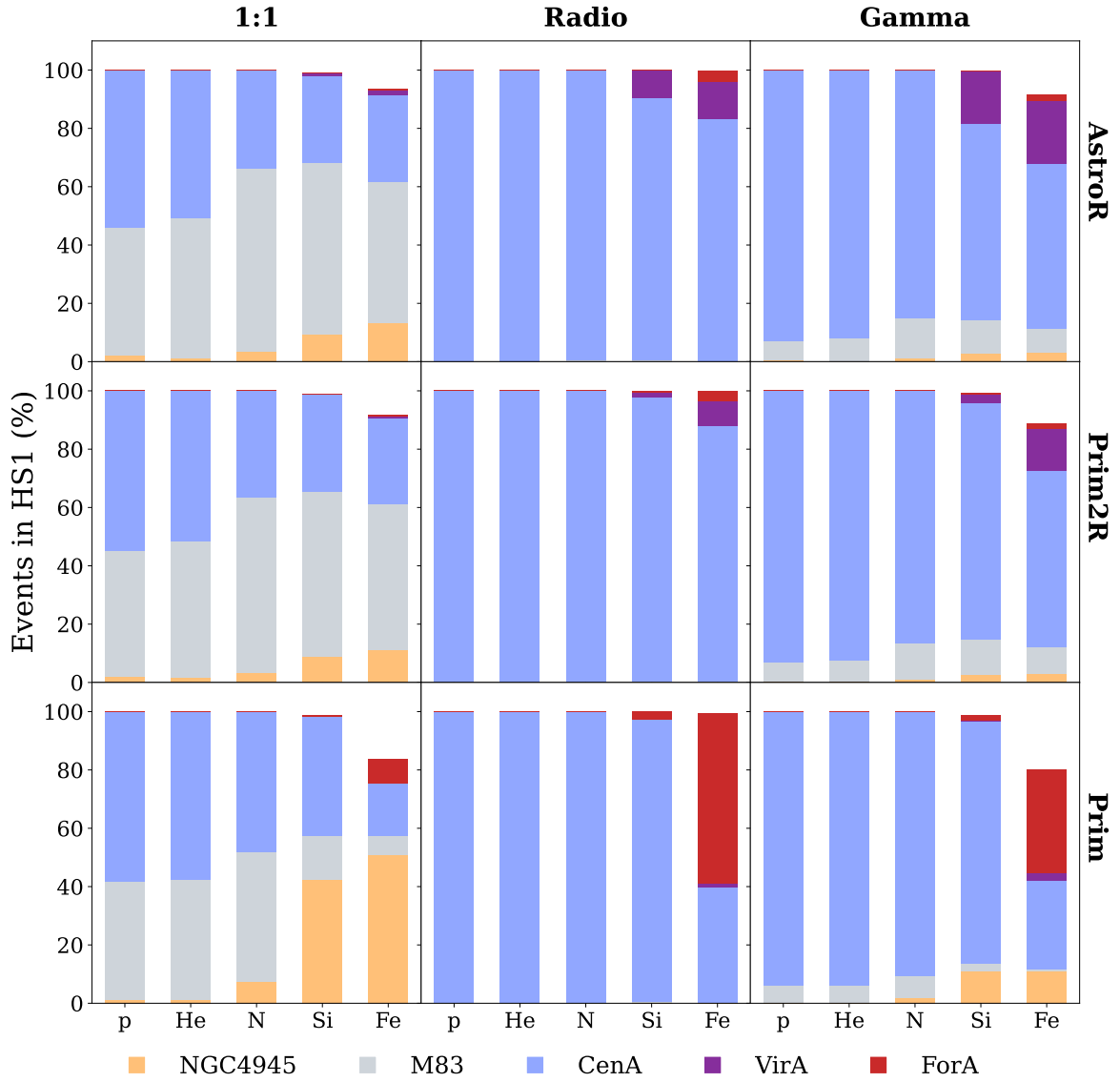


Figure 5. Contribution of sources to the HS1 separated by each UHECR luminosity proxy (1:1, Radio, and Gamma) and EGMF (AstroR, Prim2R, and Prim) models. Only sources contributing with more than 10% are showed.

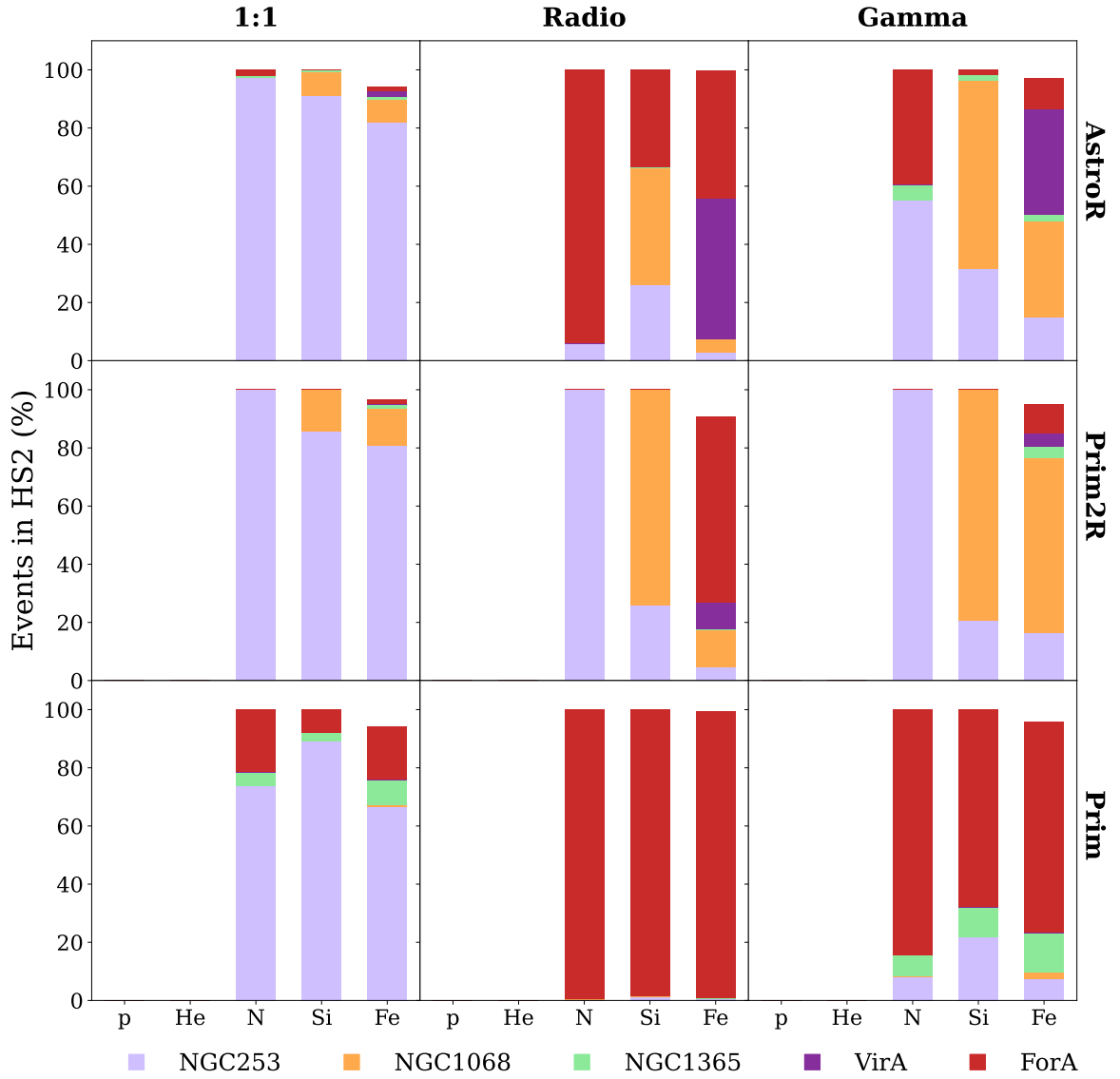


Figure 6. Contribution of sources to the HS2 separated by each UHECR luminosity (1:1, Radio, and Gamma) and EGMF (AstroR, Prim2R, and Prim) models. Only sources contributing with more than 10% are showed.

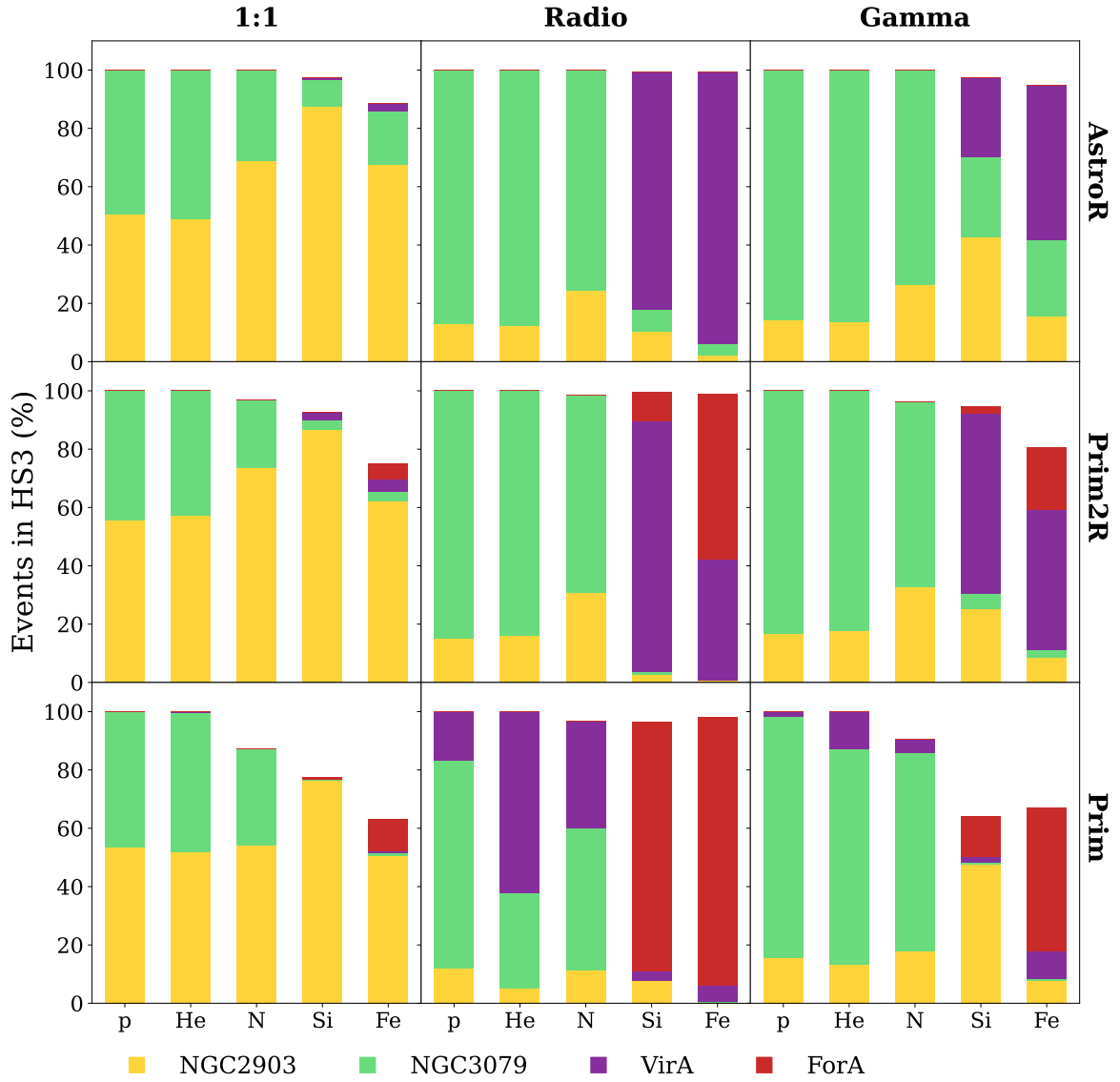


Figure 7. Contribution of sources to the HS3 separated by each UHECR luminosity (1:1, Radio, and Gamma) and EGMF (AstroR, Prim2R, and Prim) models. Only sources contributing with more than 10% are showed.

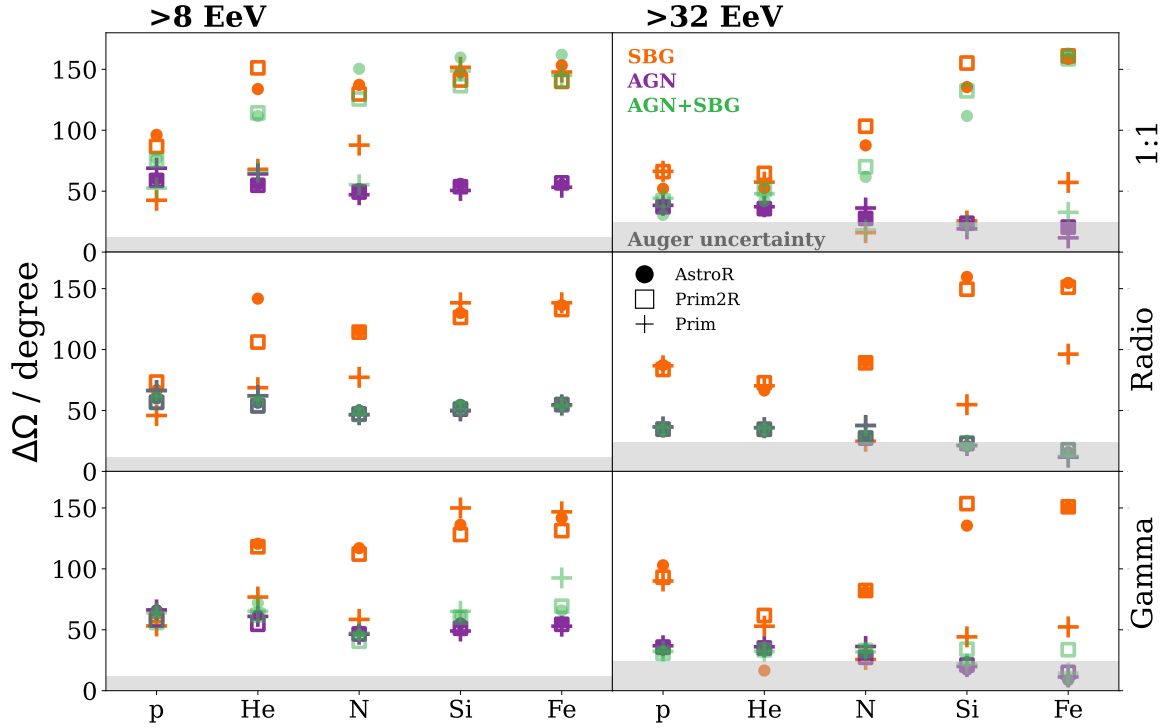


Figure 8. Angular aperture ($\Delta\Omega$) between the simulated dipole and the dipole direction measured by the Pierre Auger Observatory [30]. The data is presented as a function of the composition injected by the source (p, He, N, Si, and Fe). The left panel show the results for events with energy > 8 EeV, while the right for > 32 EeV. The top, center and bottom panels correspond to different luminosity proxies for the UHECR: identical (1:1, top), radio (center), and gamma (bottom). The colors represent different sources class (SBG, AGN, or both), while the symbols represent different EGMF models (astroR, Prim2R, and Prim). The gray region corresponds to the uncertainty of the Pierre Auger data [30] to the different energy ranges considered.

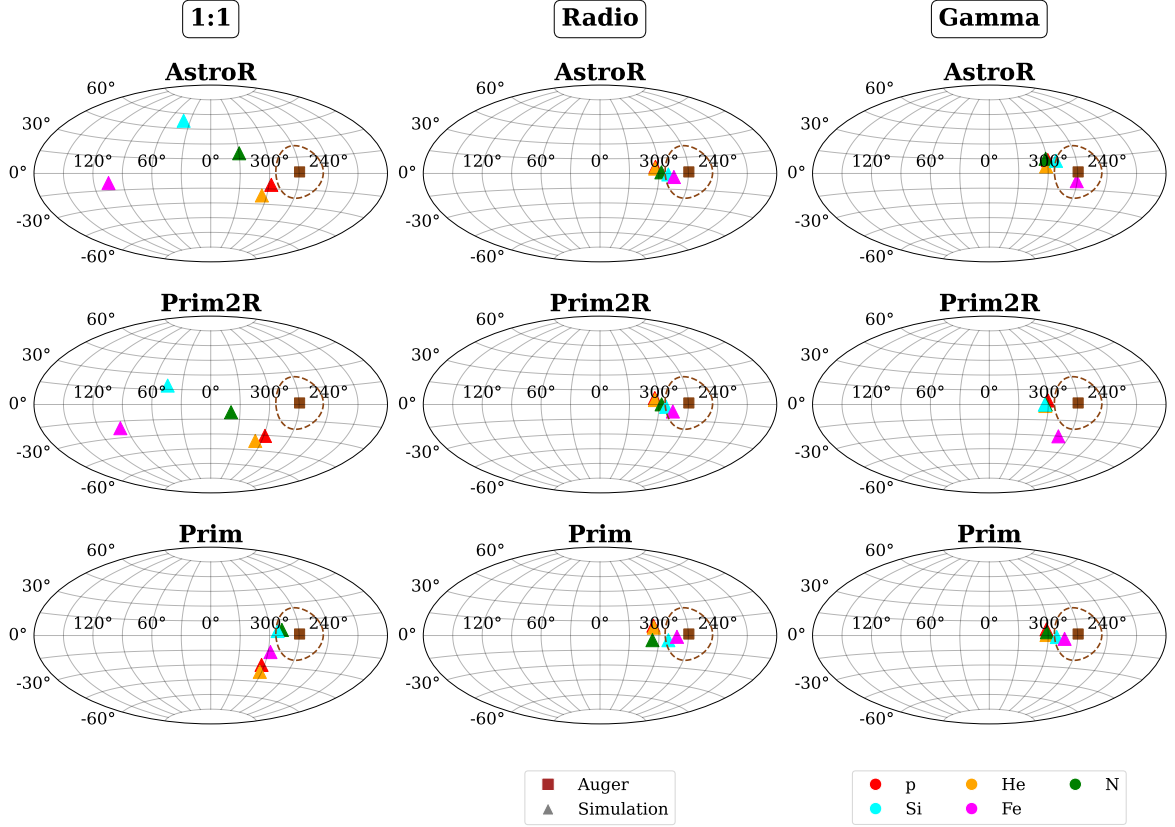


Figure 9. Dipole direction generated by events with energy above 32 EeV if SBGs and AGNs are considered sources. Each column presents different UHECR luminosities proxies: 1:1, Radio, and Gamma. Each line are shown different EGMF models: AstroR, Prim2R and Prim. The nuclei emitted by the source is mapped by colors: proton (p, red), helium (He, orange), nitrogen (N, green), silicon (Si, cyan), and iron (Fe, magenta). The brown square presents the dipole direction measured by the Pierre Auger Observatory [30]. The map is in galactic coordinates.

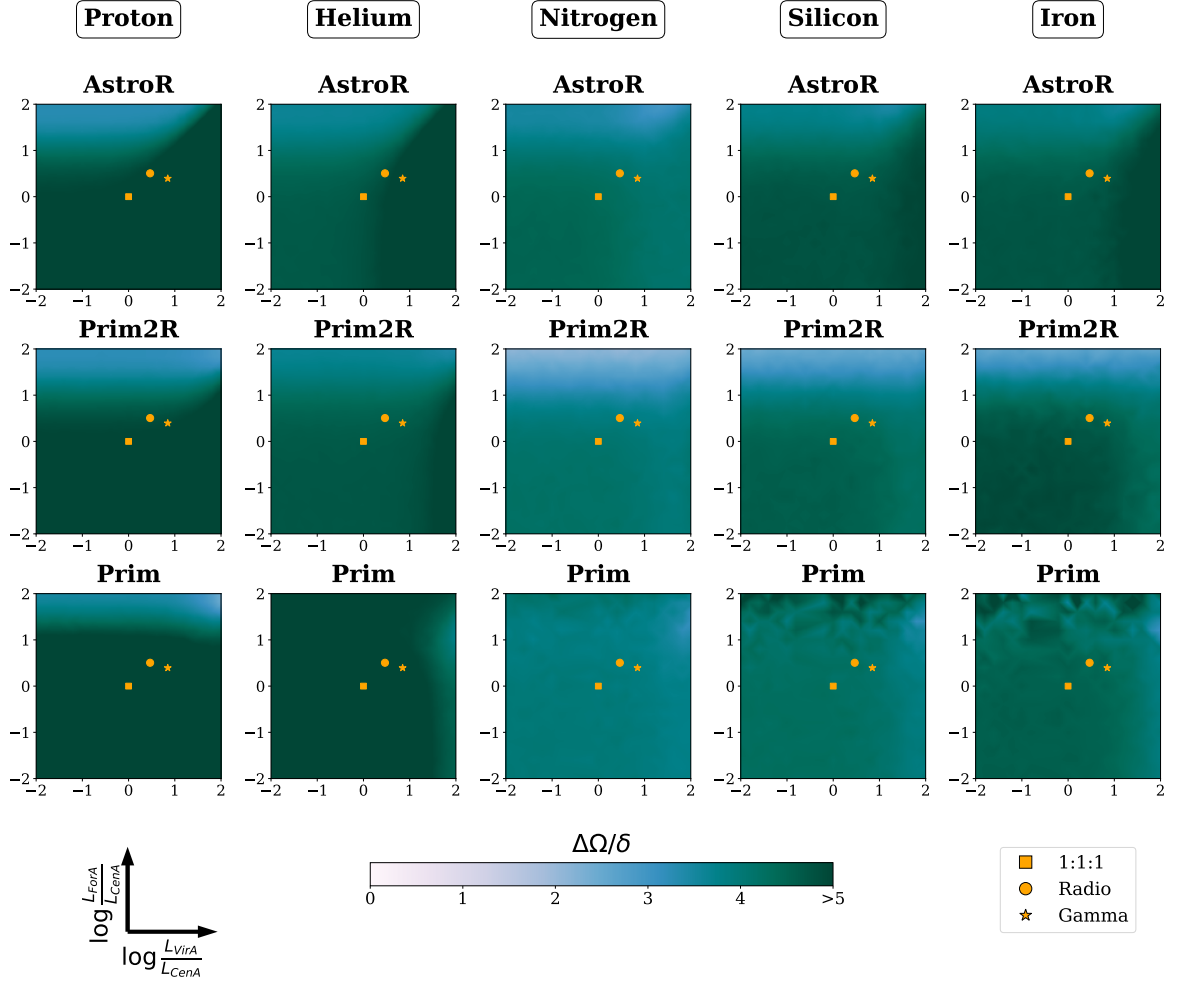


Figure 10. Normalized angular distance ($\frac{\Delta\Omega}{\delta}$) between simulated dipole direction and the direction of the dipole measured by the Pierre Auger Observatory [30] of events arriving at Earth with energy above 8 EeV. The three luminosity proxies considered in the previous sections are showed by the square (1:1:1), circle (Radio), and star (Gamma).

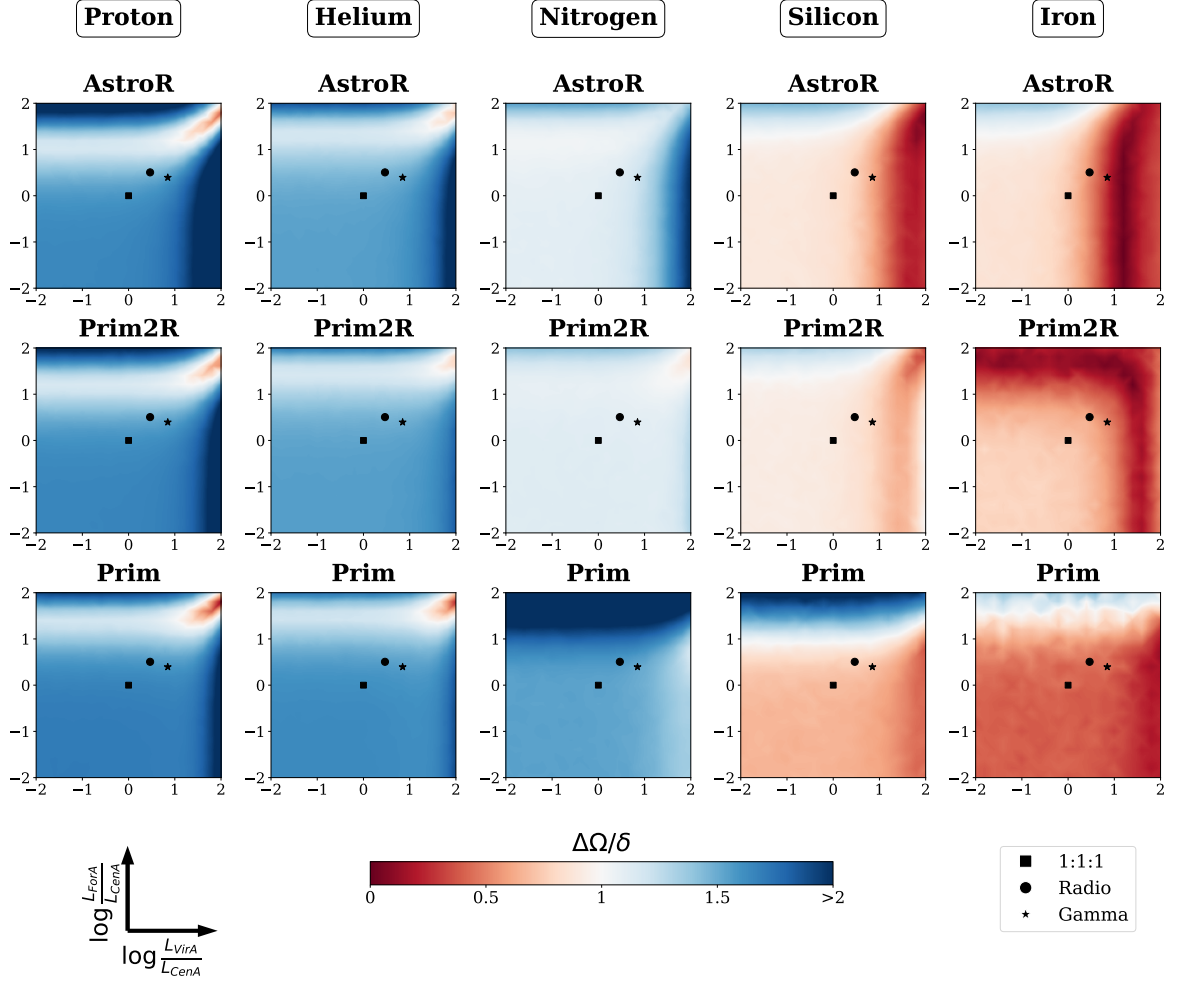


Figure 11. Normalized angular distance ($\frac{\Delta\Omega}{\delta}$) between simulated dipole direction and the direction of the dipole measured by the Pierre Auger Observatory [30] of events arriving at Earth with energy above 32 EeV. The angular distance is normalized by the uncertainty (δ) in the direction of the dipole reconstructed by The Pierre Auger Collaboration [30]. The three luminosity proxies considered in the previous sections are shown by the square (1:1), circle (Radio), and star (Gamma).

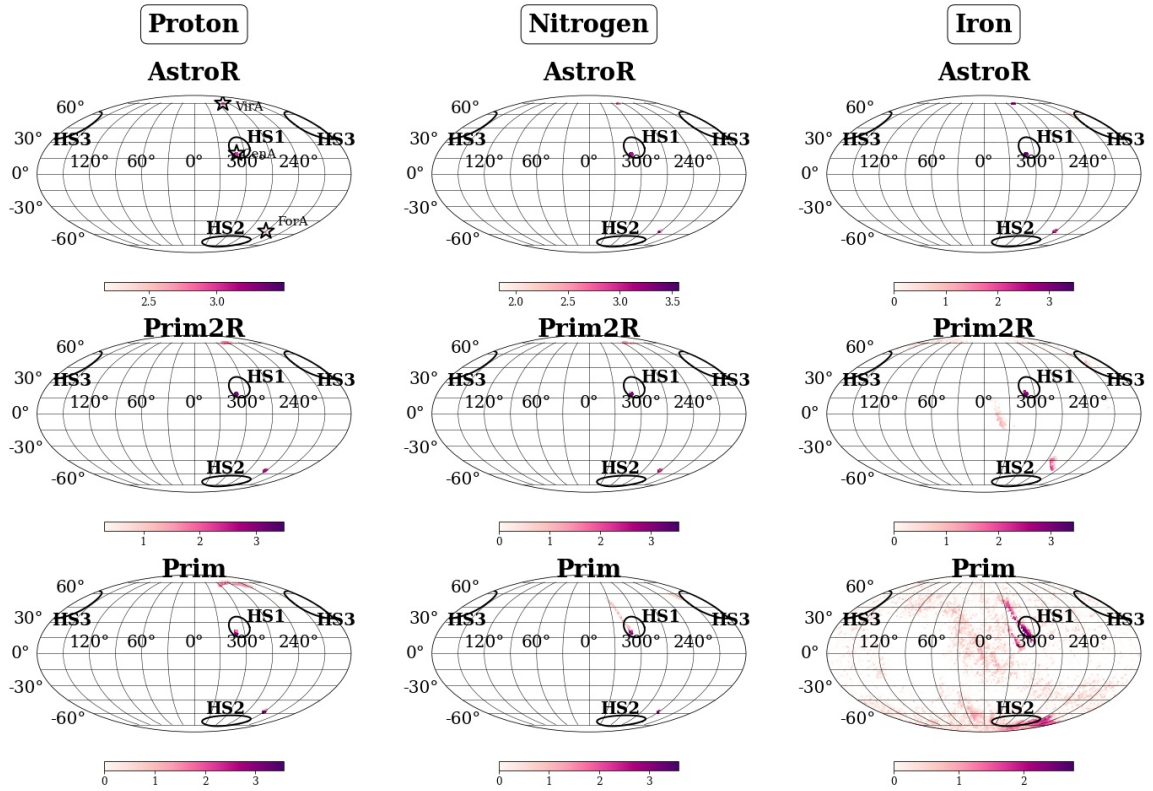


Figure 12. Arrival directions map for events with energies above 60 EeV for the AGNs in a Mollweide projection. The GMF effect is not included. The elements of figure are the same of figure 3.

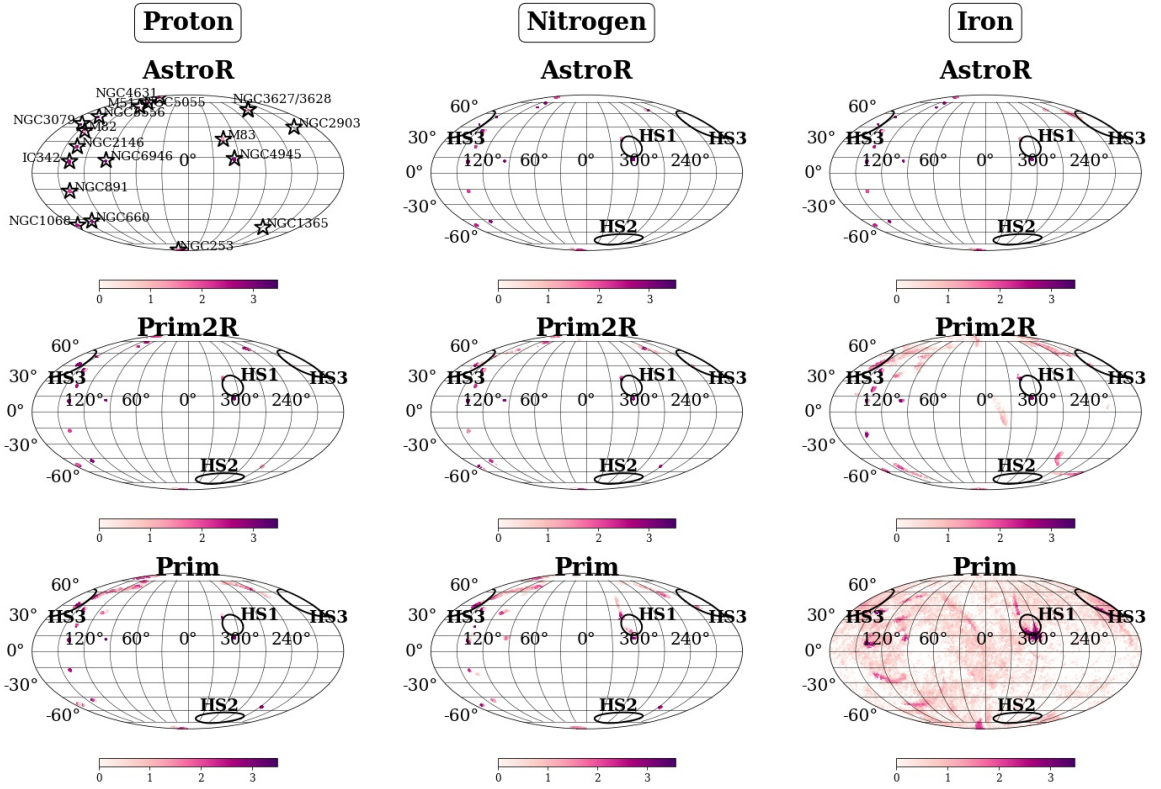


Figure 13. Arrival directions map for events with energies above 60 EeV for the SBGs in a Mollweide projection. The GMF effect is not included. The elements of figure are the same of figure 3.